

ACCEPTED PRE-PUBLICATION MANUSCRIPT

ARTICLE TITLE: Paleoproterozoic Rocks of the Belcher Islands, Nunavut: A Review of Their Remarkable Geology and Relevance to Inuit-led Conservation Efforts

AUTHORS: Brayden McDonald and Camille Partin

DOI: <https://doi.org/10.12789/geocanj.2024.51.207>

*Published in: **Geoscience Canada, Volume 51N1***

Received: April 2023

Accepted as revised: January 2024

Issue Publication: April 2024

This 'Accepted' article has been peer-reviewed and copy-edited but has not yet undergone proof-editing, layout, or pagination. Although considered published, the 'Accepted' manuscript is not the official version of record and may have undergone changes in content before being published in the Journal Issue. The article will be replaced by the published Geoscience Canada article when the 1-year subscription embargo has ended. The article's doi number is finalized and citable.

ARTICLE

Paleoproterozoic Rocks of the Belcher Islands, Nunavut: A Review of Their Remarkable Geology and Relevance to Inuit-led Conservation Efforts

Brayden McDonald and Camille Partin

*Department of Geological Sciences, University of Saskatchewan
114 Science Place, Saskatoon, Saskatchewan, S7N 5E2, Canada
E-mail: Camille.partin@usask.ca*

SUMMARY

The Paleoproterozoic Belcher Group (ca. 2.0 to 1.83 Ga) occurs on the remote Belcher Islands of Hudson Bay in Nunavut, Canada. It includes nearly nine kilometres of well-preserved siliciclastic and carbonate sedimentary rocks, deposited initially in a marginal to shallow marine setting representing one of the first true continental shelf environments on the proto-Canadian Shield. A wide variety of depositional facies exists within the Belcher Group, and it is particularly well known for its spectacular stromatolites in dolostone. In addition to these macroscopic features, two of its formations (Kasegalik and McLeary) contain intact microfossils of *Eontophysalis belcherensis*, the oldest known occurrence of cyanobacteria in the geological record. The uppermost part of the Belcher Group contains sedimentary rocks of very different character that represent a younger foreland basin that developed during development of the Trans-Hudson orogen. These younger formations (Omarolluk and Loaf) consist of a thick sequence of turbidites, overlain by arkose and other immature clastic sedimentary rocks. A defining characteristic of the Omarolluk Formation is the presence of calcareous concretions. The Omarolluk Formation shares attributes with “omars”, which are glacially transported clasts that occur both locally and further afield throughout parts of Canada and the northern United States and have helped characterize Pleistocene ice-flow trends across the continent.

The Belcher Group also includes two formations dominated by spectacular mafic volcanic rocks. The earlier episode, represented by the Eskimo Formation, reflects eruption of largely subaerial volcanic flows interpreted to represent flood basalt associated with the rifting of Archean basement during the establishment of the continental shelf. A later volcanic episode (the Flaherty Formation) is dominated by submarine pillowed basalt flows and has been assigned to varied tectonic settings, including volcanic arcs related to subduction and oceanic plateaus related to mantle plume activity and renewed rifting along the continental margin. This later volcanism marks the transition from shelf to foreland basin. Mafic sills and related intrusions (Haig intrusions) occur in the middle and lower part of the Belcher Group. Thermal and chemical interactions between mafic magma and calcareous shale generated unusual rocks that are well known in Nunavut as high-quality artisanal carving stone. The Belcher Group also contains Superior-type iron formations that have attracted past exploration interest, and minor indications of base-metal mineralization.

The Belcher Group is a unique geological entity defined by its wide variety of rock types, its superb exposures, and its potential to illustrate many important geological processes in a

formative time in Earth's history. It is also a unique microfossil paleontological resource, and its deposition brackets a crucial and much-debated interval of Precambrian atmospheric and oceanic evolution. It represents an important scientific resource in the context of understanding such changes. This general review paper highlights its most important features, discusses its potential for future research and contributes to wider discussions about its possible future role as a protected area within Nunavut.

RÉSUMÉ

Le groupe paléoprotérozoïque de Belcher (environ 2,0 à 1,83 Ga) se trouve sur les îles Belcher dans la baie d'Hudson au Nunavut, Canada. Il comprend près de neuf kilomètres de roches sédimentaires siliciclastiques et carbonatées bien préservées, déposées initialement dans un milieu marin marginal à peu profond, représentant l'un des premiers véritables environnements de plateau continental du proto Bouclier canadien. Une grande variété de faciès de dépôt existe au sein du groupe de Belcher, et celui-ci est particulièrement bien connu pour ses stromatolithes spectaculaires dans la dolomie. En plus de ces caractéristiques macroscopiques, deux de ses formations (Kasegalik et McLeary) contiennent des microfossiles intacts d'*Eontophysalis belcherensis*, la plus ancienne occurrence connue de cyanobactéries dans les archives géologiques. La partie supérieure du groupe de Belcher contient des roches sédimentaires de caractère très différent qui représentent un bassin d'avant-pays plus jeune qui s'est formé au cours du développement de l'orogène trans-hudsonien. Ces formations plus jeunes (Omarolluk et Loaf) sont constituées d'une épaisse séquence de turbidites, recouvertes d'arkose et d'autres roches sédimentaires clastiques immatures. Une caractéristique déterminante de la formation d'Omarolluk est la présence de concrétions calcaires. La formation d'Omarolluk partage des attributs avec les « omars », qui sont des clastes transportés par les glaciers qui se retrouvent à la fois localement et plus loin dans certaines parties du Canada et du nord des États-Unis et qui ont contribué à caractériser les directions d'écoulement glaciaire du Pléistocène à travers le continent.

Le groupe de Belcher comprend également deux formations dominées par de spectaculaires roches volcaniques mafiques. L'épisode le plus ancien, représenté par la formation d'Eskimo, reflète l'éruption de coulées volcaniques en grande partie subaériennes interprétées comme représentant des basaltes de plateau associés au rift du socle archéen lors de l'établissement du plateau continental. Un épisode volcanique ultérieur (la formation de Flaherty) est dominé par des coulées sous-marines de basalte en coussins et a été attribué à divers contextes tectoniques, notamment des arcs volcaniques liés à la subduction et des plateaux océaniques liés à l'activité de panaches mantelliques et à une nouvelle phase de rift le long de la marge continentale. Ce volcanisme ultérieur marque la transition du plateau au bassin d'avant-pays. Des filons-couches mafiques et des intrusions associées (intrusions de Haig) sont présents dans la partie moyenne et inférieure du groupe de Belcher. Les interactions thermiques et chimiques entre le magma mafique et les schistes calcaires ont généré des roches inhabituelles qui sont bien connues au Nunavut comme des pierres à sculpter artisanales de haute qualité. Le groupe de Belcher contient également des formations ferrifères du type du lac Supérieur qui ont suscité un intérêt en matière d'exploration dans le passé, ainsi que des indications mineures de minéralisation en métaux communs.

Le groupe de Belcher est une entité géologique unique définie par sa grande variété de types de roches, ses superbes affleurements et son potentiel à illustrer de nombreux processus géologiques importants à une époque fondatrice dans l'histoire de la Terre. Il constitue

également une ressource paléontologique de microfossiles unique, et ses dépôts se situent dans une période cruciale et très controversée de l'évolution atmosphérique et océanique du Précambrien. Il représente une ressource scientifique importante dans le contexte de la compréhension de tels changements. Cet article de synthèse générale met en lumière ses caractéristiques les plus importantes, discute de son potentiel pour de futures recherches et contribue aux discussions plus larges sur son rôle futur éventuel en tant que zone protégée au sein du Nunavut.

Traduit par la Traductrice

INTRODUCTION

The Belcher Islands (Inuktitut: ᓴᓇᓴᓴᓴ) are in the southeast corner of Hudson Bay in Nunavut, northern Canada (Fig. 1). The Belcher Islands are within the proposed protected area of Qikiqtait, a community-based, Inuit-led conservation program initiated by the community of Sanikiluaq, Nunavut, in conjunction with the Sanikiluaq Hunters and Trappers Association, the Arctic Eider Society, and the Qikiqtani Inuit Association (Haycock-Chavez 2021; Sanikiluaq Qikiqtait Steering Committee 2021). The Qikiqtait Protected Area project aims to protect the Belcher Island archipelago, which has cultural, ecological, biological, and geological significance. The project aims to build the framework for a conservation economy while adding levels of protection to the entire Belcher Islands terrestrial and marine region.

The Belcher archipelago is a region of remarkable geology that is in many ways unparalleled in the Canadian Shield. The islands provide superb ice-scoured bedrock exposures along hundreds of kilometres of convoluted shorelines, which reveal Paleoproterozoic sedimentary and volcanic rocks that are remarkably well preserved. These are collectively known as the Belcher Group and are most extensively described by Jackson (2013) and Ricketts (1979), which are important sources of information for this overview in addition to our own field work in the Belcher Group that began in 2018. The Belcher Group is unique in the Hudson Bay region, which is elsewhere dominated by flat-lying Paleozoic sedimentary rocks. The Belcher Group provides a window into the distant geological past, when ancient oceans were dominated by single-celled organisms such as cyanobacteria, rather than the diverse multicellular invertebrate and vertebrate animals of modern oceans. Fossilized cyanobacterial mats and mounds, called *stromatolites*, are common in carbonate sedimentary rocks of the Belcher Group and, in some formations, are spectacular. Stromatolites are rare in the oceans today, but persist in hypersaline settings such as Shark Bay, Australia (Suosaari et al. 2022) or in open marine settings such as those found in the Highborne Cay reef system and Exuma Cays of the Bahamas (Andres and Reid 2006). However, they were the dominant life-forms billions of years ago, and were responsible for fundamental changes in the wider Earth system. The oceans of two billion years ago had a different chemical composition from those of today. Today, the oceans are well-oxygenated through equilibration with our atmosphere and contain many elements that provide key nutrients for life as we know it. In contrast to today, the ocean in which the Belcher Group was deposited lacked many of these characteristics and was instead poorly oxygenated (e.g. Partin et al. 2013; Hodgskiss et al. 2019a; Hodgskiss and Sperling 2022; Lyons et al. 2021; Partin 2023). Although there are a few geological and geochemical indicators that help support the lack of available oxygen in the oceans during this time (e.g. variations in $\delta^{13}\text{C}$, redox-sensitive minerals and elements, etc.) a major lithological indicator of oxidation state is the presence of granular iron formations (GIFs) within the Belcher Group. Iron formations are a specific product of poorly and partly oxygenated conditions that require dissolved iron in a

reduced chemical state (Fe^{2+}) to be mobilized and eventually form iron solids via oxidation. Iron formations are thus an important hallmark of the progressive and episodic oxygenation of Earth's earliest oceans (Konhauser et al. 2017). The iron formations of the Belcher Group are part of a global development of such iron formations during the early Paleoproterozoic. These unusual rocks are rare in the geological record after about 1.84 Ga (e.g. Poulton et al. 2010). The Belcher Group, and correlative sequences elsewhere in North America, are part of this final episode of iron formation development (e.g. Konhauser et al. 2017).

About 20 to 30% of the total thickness of the Belcher Group consists of mafic volcanic rocks of basaltic affinity. These were erupted during two different intervals and are distinctly different in character. The first volcanic episode interrupted carbonate deposition associated with the Kasegalik Formation. A zircon U–Pb age of 2015 ± 1.8 Ma from a tuff bed located within the uppermost unit of the Kasegalik Formation places an approximate age constraint on the start of volcanism (Hodgskiss et al. 2019a). This period of volcanism is attributed to rifting along the Superior margin during the expansion of the Manikewan Ocean and manifested as a series of voluminous subaerial continental flood basalt flows (Jackson 1960, 2013; Legault et al. 1994). The second volcanic episode produced a series of tholeiitic basalt units, represented by submarine flows of the Flaherty Formation and the feeder dykes of the Haig intrusions (Jackson 2013). Emplacement of the Flaherty Formation volcanic rocks denotes a period of tectonic change along the Superior craton margin and marks a switch in depositional environment for the Belcher Group. A baddeleyite U–Pb age of 1870 ± 3 Ma (Hamilton et al. 2009) from the Haig sills, which occur primarily at the base of the Flaherty Formation as well as lower in the stratigraphy, suggests the second phase of volcanism could be linked to the development of volcanic arcs during the closing of the Manikewan Ocean that occurred between ca 1.92 Ga and 1.83 Ga (Corrigan et al. 2009). Alternatively, the Haig sills could be a product of a mantle plume associated with the Pan-Superior large igneous province as proposed in Ernst and Bell (2010). In either case, the Flaherty volcanic flows mark a period of significant change for the Belcher Group with respect to the tectonic environment and the depositional environment. The following period of sedimentation, represented by the Omarolluk Formation, was no longer marked by relatively slow deposition characteristic of passive margins but instead was dominated by rapid deposition within a newly forming foreland basin.

Sedimentary rocks that make up the remaining 70–80% of the Belcher Group represent a long history of about 185 m.y., with several discrete stages of evolution. Deposition initially began in a terrestrial fluvial environment, which transitioned to marginal marine and tidal beach environments, and then to a deeper water, offshore marine environment before eventually returning to oscillating fluvial, tidal and shallow marine conditions. For the most part, this sedimentation was dominated by carbonate rocks; ancient equivalents of those that form today in low latitude waters. Large reefs built by stromatolites were an important component of these ancient shorelines, and a brief period of iron formation deposition developed, possibly in an associated barred basin (Ricketts 1979). The youngest sedimentary rocks, after the second volcanic episode, formed in deeper waters in a submarine fan that eventually evolved to a fluvial setting. This younger sequence is dominantly of clastic origin, derived by erosion from varied sources. These changes in depositional environment record the breakup of an early continental region by rifting and establishment of a stable continental shelf, followed by subsidence and the arrival of detritus from other regions that had formerly been open ocean. These events were broadly part of the protracted tectonic assembly of the various crustal blocks that now constitute the core of the Canadian Shield. These processes are a record of early plate tectonics operating

on our planet and are believed to represent the assembly of the first true supercontinent on Earth (Evans and Mitchell 2011), appropriately named *Nuna* (“land” in Inuktitut). The Belcher Islands are a small part of one of the first globally extensive orogenic belts to be generated in Earth’s long history. The final collision of continental blocks (on a scale consistent with that of the modern Alpine–Himalayan chain) is recorded in the complex fold structures that determine the very shape of the islands (Fig. 2), and the structural geology of the Belcher Group is just as striking as their record of sedimentation and volcanism (e.g. Jackson 2013).

The Belcher Islands are within a proposed protected area envisioned by *Qikiqtait*, led and championed by the community of Sanikiluaq, Nunavut. The Qikiqtait project ultimately aims to protect the Belcher archipelago, which has great cultural, historical, and ecological significance in addition to the geological aspects summarized in this paper. The project hopes to build the framework for a more conservation-oriented economy by adding several levels of protection to the entire Belcher Islands terrestrial and marine regions. In the proposed Nunavut Land Use Plan (LUP; Nunavut Planning Commission 2021) the Belcher Islands are assigned to a *limited use* land category, largely to conserve migratory bird habitats and other marine wildlife. If adopted, such designation would preclude various industrial activities including mineral resource development beyond existing licenses. However, the islands are not yet part of a formally proposed future park or conservation area. As of publication, the Nunavut LUP has not been formally accepted by the territorial or federal governments, or by the other signatories to the LUP process.

In addition to land-based conservation efforts, Inuit-led conservation is crucial to the success of federal marine conservation efforts. With the success of designating High Arctic marine conservation with the Tallurutiup Imanga National Marine Conservation Area and Tuvaijuittuq Marine Protected Area in 2019, further work to advance marine conservation projects in the Sarvarjuaq and Qikiqtait marine areas remains significant because these two areas will contribute approximately 2% towards the “25 per cent by 2025” marine conservation target set by the government of Canada (House of Commons Standing Committee on Fisheries and Oceans 2023). If successful, the Qikiqtait marine area would become a Marine Protected Area. In its 2023 Marine Protected Area Protection Standard, Canada defined that this standard would prohibit the exploration, development, and production of both oil and gas and mineral resources; disposal of waste and other matter; and mobile, bottom contact, trawl or dredge gear (though trap-based fisheries are excluded). This policy has been endorsed by Fisheries and Oceans Canada, Environment and Climate Change Canada, Parks Canada, Natural Resources Canada, Crown-Indigenous Relations and Transport Canada. Efforts continue towards this goal on various federal, territorial and local scales, including a new community-learning centre in Sanikiluaq. More information on Qikiqtait can be found at <https://qikiqtait.ca/>.

This paper evolved from a technical review of the geology and wider geoscientific context of the Belcher Group that was prepared as part of the information gathering phase of the Qikiqtait proposals. This activity is linked to our own ongoing geoscience research in the area, but the paper itself is primarily a review and synthesis of previous work, notably by Geological Survey of Canada mapping Jackson (1960, 2013) and subsequent studies by Hans Hofmann, Brian Ricketts, Al Donaldson, and many others. Some of the source material is of a specialized nature, but is presented here at a more general level, with the intention of reaching a wider geoscience readership. For a more complete discussion of rock units within the Belcher Group, or specific problems related to its evolution and wider context, readers are referred to the numerous publications in the references. The wider objective of this paper is to provide an informative and

accessible holistic review of this remarkable and influential area of Canadian Shield geology, which to date has not been attempted.

The remainder of the paper follows the conventions of geological reports and assumes knowledge of geological concepts and some aspects of stratigraphy, sedimentology and paleontology. First, the regional geological setting of the Belcher Group is summarized, with reference to modern plate tectonic models for this interval of Precambrian time (part of the Paleoproterozoic; ca. 2.5 Ga–1.6 Ga). This is followed by more detailed treatment of the Belcher Group, including stratigraphy, depositional environments, age constraints, depositional phases and structural and metamorphic aspects. Economic and cultural geological resources including iron ore deposits and aspects of well-known artisanal carving stone deposits are discussed. The final section of the paper is a more focused review of the rare, and in some cases unique, geological features of these rocks. These include their exceptional preservation, a unique-in-time microfossil record and great relevance to understanding the early evolution of Earth's atmosphere and oceans through their sedimentary record and geochemistry.

GEOLOGICAL SETTING

Regional Geology and Tectonic Context

The Belcher Islands in southeastern Hudson Bay are part of the Precambrian Canadian Shield (Fig. 1). Regionally, they form part of the Trans-Hudson orogen, which is an extensive Paleoproterozoic orogenic belt that separates the Archean Superior Province from other Archean and Paleoproterozoic regions that underlie much of Arctic Canada and adjacent Greenland (Hoffman 1988; Corrigan et al. 2009; St-Onge et al. 2009) (Fig. 1; note that later Precambrian and Phanerozoic cover rocks are omitted for clarity). The Trans-Hudson orogen records the development of the Manikewan Ocean, followed by its progressive closure as oceanic crust was subducted and destroyed, leading to collision of the surrounding Archean continental blocks. More extensive discussion of these events is provided by several important papers (e.g. Ansdell 2005; Corrigan et al. 2009; Corrigan et al. 2021) and the following account summarizes only some key aspects.

It is proposed that a large Archean continental region known as *Kenorland* underwent protracted breakup between ca. 2.45 and 2.1 Ga, leading to final fragmentation at ca. 2.1–2.0 Ga (Aspler and Chiarenzelli 1998). Growth of the Manikewan Ocean ca. 2.1–1.92 Ga was enabled through continued seafloor spreading as well as eustatic (global) sea level rise leading to the development of thick passive margin sequences along the margins of the newly fragmented Archean blocks (e.g. those on the Superior craton, Belcher Group, Richmond Gulf Group, and Povungnituk Group; Ricketts and Donaldson 1981; Chandler and Parrish 1989; St-Onge and Lucas 1991; St-Onge and Ijewliw 1996). This period of relative quiescence along the Superior margin coincides with most of the Belcher Group depositional window and facilitated protracted development of stable carbonate platforms and shelf to slope marine depositional settings. However, a dramatic change occurred with the next stage from stable passive margin deposition to the development of a foreland basin during the deposition of upper Belcher Group units, which occurred in the context of the ca. 1.9–1.8 Ga Trans-Hudson orogenic events (e.g. Corrigan et al. 2021).

The collision and amalgamation of Archean cratons, microcontinents, and volcanic island arcs in the Trans-Hudson orogen was a pivotal event in the formation of Laurentia (Fig. 1) and the present location of the Hudson Bay region was at its very centre. The earliest stages of the

Manikewan Ocean closure ca. 1.92–1.89 Ga saw the amalgamation of the Rae and Hearne cratons along the Snowbird Tectonic Zone (Berman et al. 2007; Corrigan et al. 2009; Regis et al. 2021); the accretion of numerous volcanic arcs to the newly formed Churchill Province (e.g. Reindeer orogeny ca. 1.88–1.85 Ga) and the collision between Meta Incognita and the eastern Rae craton (Foxe orogeny ca. 1.89 Ga). Most of these earlier tectonic events had little effect on the deposition of the Belcher Group; it is likely they were occurring on the other side of the Manikewan Ocean. This however changed ca. 1.87 Ga as terrane accretion along the southern edge of the Churchill Province began with the obduction of the Watts Group ophiolite and Parent/Spartan volcanic arc complex onto the northern margin of the Superior craton (St-Onge et al. 2000; Corrigan et al. 2021). Continued closure of the Manikewan Ocean influenced the Belcher Group starting ca. 1.87 Ga with the extrusion of the Flaherty Formation volcanic flows and the initiation of a submarine fan succession interpreted to represent a foreland basin (Ricketts 1981; Jackson 2013).

The terminal collision of the Superior craton and Churchill Province ca. 1.83 Ga created a mountain belt interpreted to be analogous in size to the modern Himalaya mountain belt (Weller and St-Onge 2017) and was essential to forming the core of Laurentia. The resulting ~4000 km-long continent–continent collisional belt extends from the modern day western United States to Greenland and Scandinavia and played a major role in the development of the Nuna supercontinent (Evans and Mitchell 2011).

The outcome of this long and complex geological story was the collision between the Superior craton and Archean cratonic blocks now represented by the Rae and Hearne cratons and other areas in the Arctic that have an Archean heritage (Fig. 1). The region to the north, west and east (present coordinates) was widely affected by metamorphism, deformation, and magmatism whereas much of the interior Superior craton remained unaffected, preserving its earlier history (e.g. Ansdell 2005; Corrigan et al. 2009, 2021; Percival 2007). Other parts of northern Canada, such as the Quebec–Labrador area (termed the Southeastern Churchill Province) are also part of this complex story of continental dispersion and re-assembly (e.g. Corrigan et al. 2021). The Cape Smith belt and the New Quebec orogen (Fig. 1) both contain volcanic–sedimentary sequences some of which are time-correlative with the Belcher Group and defined as the Circum-Superior belt around the margin of the Superior craton (e.g. Baragar and Scoates 1987; Skipton et al. 2023). Time-correlative sedimentary and metasedimentary rocks in Labrador and Quebec produce most of Canada’s iron ore (Gross 2009). Paleoproterozoic sedimentary rocks in Minnesota and nearby regions, which host the world class iron ore deposits of the Mesabi Range (Laznicka 2014), are also time-correlative.

In the Belcher Islands and adjacent regions of Hudson Bay, there are two main Precambrian geological components, the Archean basement rocks and the sedimentary–volcanic rocks of the Richmond Gulf and Nastapoka groups (mainland of Quebec and nearby islands; Chandler 1984, 1988) and the Belcher Group in Nunavut. The Archean basement rocks are not exposed on the Belcher Islands but assumed to exist at depth. Arkosic sandstone of the basal Richmond Gulf Group, however, rests unconformably upon Archean basement rocks. The tholeiitic basalt flows and alluvial–fluvial–lacustrine sandstone and mudstone of the Persillon and Pachi formations and conglomerate and sandstone of the overlying Quingaaluq Formation are interpreted to represent early rifting of the Superior craton ca. 2025 Ma (Chandler and Parrish 1989).

The siliciclastic and carbonate rocks of the Belcher Group represent deposition on a passive margin to foreland basin, with the lower volcanic unit (Eskimo Formation) representing a rift-related stage and the upper volcanic unit (Flaherty Formation) representing a foredeep stage

(Dimroth et al. 1970; Jackson 2013). Paleocurrent indicators from the Belcher Group suggest that there was a reversal of sedimentary provenance from dominantly south-southwest to north-northwest (present coordinates) in the upper part of the sequence (Ricketts 1979, 1981). This suggests that the accretion of intra-oceanic terranes during closure of the Manikewan Ocean had initiated by this time, and that these terranes were being exhumed and provided eroded detritus for the upper part of the Belcher Group.

General Geology of the Belcher Islands and Adjacent Areas

Paleoproterozoic supracrustal rocks are present along a collection of island chains in eastern Hudson Bay including the Belcher, Ottawa, Sleeper, and Nastapoka Islands (Fig. 2). The Belcher Group is the most extensive of these, and its geology is illustrated in Figure 2, simplified from the work of Jackson (2013). The stratigraphy of the Belcher Group is illustrated in Figure 3, simplified from Ricketts (1979) and Jackson (2013).

The geological history of the Belcher Group began prior to ca. 2019 Ma with the deposition of the Kasegalik Formation in a fluvial to marginal marine (shoreline) environment in an overall extensional tectonic setting. Note that the older Richmond Gulf Group is also dominated by clastic rocks of fluvial origin. The main part of the Belcher Group is composed primarily of mixed carbonate and siliciclastic sedimentary rocks that are punctuated by volcanic rocks erupted in two episodes. The rift-related basalts of the Eskimo Formation (ca. 2015 Ma) overlie the Kasegalik Formation (Fig. 3). The overlying sedimentary rocks of the middle Belcher Group are divided into nine formations, dominated by carbonate rocks with intervening siliciclastic rocks, and eventually capped by the iron formations of the Kipalu Formation (Fig. 3; more discussion below). These represent a return to undisturbed passive margin sedimentation after the first volcanic episode, but cyclic sedimentary patterns suggest a variety of depositional settings from fluvial to offshore marine. The iron-rich rocks of the Kipalu Formation are overlain by a second accumulation of submarine tholeiitic basalt flows represented by the Flaherty Formation. These volcanic rocks are overlain by clastic sedimentary rocks of the Omarolluk and Loaf formations (Fig. 3), which are lithologically distinct from the mixed carbonate–siliciclastic assemblage beneath the Flaherty Formation. The uppermost Belcher Group consists of shale and turbidite units deposited in deeper water settings, overlain by a mixture of immature sedimentary rocks including arkose and conglomerate in shallow water settings.

The Belcher Islands were covered in ice during the Pleistocene by the Laurentide Ice Sheet, which covered all of Canada. The Keewatin and Quebec–Labrador sector of the Laurentide Ice Sheet was responsible for flow over the Belcher Islands (Dyke et al. 2002) that produced erosional features such as glacial striae, chatter marks, roches moutonnées, as well as crag and tail structures that indicate dominantly southwesterly movement of ice (e.g. Jackson 1960; Ricketts 1979). While Ricketts (1979) showed that about 80% of the glacial striae were southwest-directed, other glacial structures indicate southwest to north, northeast and east directions. Ricketts (1979) interpreted these to cut the southwest-trending structures, though Jackson (2013) did not observe clear overprinting relationships. In either case, the dominantly southwesterly ice flow direction is consistent with the occurrence of distinctive “omar” glacial till clasts that occur in several provinces including Manitoba, Ontario, Saskatchewan, and Alberta, as well as the northern United States, including Minnesota, Wisconsin, North Dakota, South Dakota, Illinois, and Michigan (Prest et al. 2000). The presence of omars documented in northern Manitoba, including the Hudson Bay lowlands, is consistent with southwest-trending ice flow directions from the Quebec dome across the Belcher Islands, though it is noted that the

Laurentide Ice Sheet history is complex and omars were likely redistributed in subsequent glacial advances and retreats (e.g. Gauthier et al. 2019). Glacial till clasts defined by a low-metamorphic grade wacke with characteristic buff weathering, rounded calcareous concretions were defined as omars by Prest (1990) and Prest et al. (2000), and are believed to be sourced from the Omarolluk Formation. This interpretation was bolstered by the presence of another unique clast type consisting of oolitic jasper, thought to be sourced from the Kipalu Formation (Prest 1990). The omar hypothesis requires more testing and is currently the subject of a research project (Pastula and Partin 2023).

Previous Research in the Belcher Islands

The geology of the Belcher Islands was first explored and documented by Flaherty (1918) and Moore (1918), followed by Young (1922). The earliest cartography of the Belcher Islands is attributed to an Inuit leader named George Weetaltuk; his remarkably accurate sketch map of the island archipelago, completed in 1910, led Robert Flaherty to explore the islands starting in 1914. These early reports make fascinating reading, and certainly convey the arduous nature of early geological field work in a region that remains remote to this day. They also contain thoughtful and detailed descriptions and discussions that have stood the test of time, establishing the fundamentals of stratigraphy. Descriptions of stromatolites from the Islands (Moore 1918) provided strong evidence for the existence of ‘low forms of life’ in the depths of the Precambrian, and cell-like structures were first observed under the microscope at this time. The presence of possibly important iron ore deposits was confirmed, but they were not then considered viable. The Belcher Mining Corporation Ltd. began more systematic exploration in 1955, and later provided important geological information that aided in the initial geological mapping efforts of Jackson (1960). Led by Garth Jackson, the Geological Survey of Canada mapped the Belcher Islands from 1958 to 1959, resulting in the first published geological map of the Belcher Islands, which subdivided the Belcher Group into 14 units (Jackson 1960). This was also a monumental effort, and Garth Digby Jackson (1929–2021) would become a prominent Geological Survey of Canada geologist after his first field assignment, eventually becoming well known for his work on Baffin Island and across the Arctic (Frisch 2021). Jackson never lost his interest in the Belcher Islands, and as an octogenarian, he completed a more detailed memoir integrating the early 1958–1959 field work with much subsequent research (Jackson 2013). This document remains a truly invaluable resource for modern researchers. Numerous BSc, MSc, and PhD theses were completed from 1959 to present from a variety of institutions, aimed generally at smaller areas or specific problems. A seminal paper by Hofmann and Jackson (1969) documented microfossils (cyanobacterial cells) associated with stromatolites, and is still of great interest today, as it led to insights about the history of oxygenic photosynthetic organisms and the evolutionary trajectory of eukaryotes (e.g. Butterfield 2015; Hodgskiss et al. 2019b). Subsequent papers involving Hans Hofmann (e.g. Hofmann 1974, 1976; Golubic and Hofmann 1976; Hofmann and Jackson 1987) documented diverse stromatolite morphologies and microfossil morphotypes dominated by cyanobacteria cells or colonies of cells. Although stromatolitic structures are documented in the earlier parts of the Precambrian, these examples still represent the oldest cyanobacterial cells preserved in the geological record. Several papers led by Brian Ricketts were pivotal to understanding the stratigraphy and depositional environments of the Belcher Group (e.g. Ricketts 1979, 1981, 1983). Important work on the Eskimo and Flaherty formations (e.g. Ricketts et al. 1982; Legault et al. 1994; Arndt and Todt 1994) determined their volcanic facies (environments), examined their geochemistry, and

speculated on their tectonic setting. Dimroth et al. (1970), Chandler (1984), and Ricketts and Donaldson (1981) all contributed similar investigations aimed at understanding links between volcanism and regional tectonics. A recent paper by Ciborowski et al. (2017) suggested connections between mafic volcanism in the Belcher Group and a “large igneous province” related to mantle plume activity around the Superior craton. More recent research on the Belcher Group has focused on geochemical patterns that allow reconstruction of ancient ocean chemistry, especially its oxidation state (e.g. Hodgskiss et al. 2019a, b) and further discussion of tectonic setting and models (e.g. Corrigan et al. 2021). The microfossil record of the Belcher Group also continues to attract research (e.g. Dodd et al. 2018; Gabriel et al. 2021). An updated geological map at 1:125 000 scale accompanies the memoir of Jackson (2013) covering all the islands and is presented here in simplified form as Figure 2. Figure 3 illustrates the stratigraphy of the Belcher Group after Ricketts (1979) and is used as a framework for the following discussion of units.

Stratigraphy of the Belcher Group

The Belcher Group consists of 14 geological formations, and also gabbro sills associated with the last pulse of volcanic activity represented by the Flaherty Formation basalt (Fig. 3). Similar dykes and sills occur in other parts of the underlying stratigraphic sequence. The Belcher Group ranges in thickness from less than 2 km on Tukarak Island in the east to about 9 km on Kugong Island in the west (Legault et al. 1994; Jackson 1960, 2013). Specific formations are discussed in detail below, with emphasis on rock types, depositional environments, and characteristic structures. The following descriptions are simplified and adapted mostly from those of Hofmann and Jackson (1969), Ricketts (1979, 1981, 1983), Ricketts and Donaldson (1981, 1989), Ricketts et al. (1982), Legault et al. (1994), and Jackson (2013), supplemented by recent observations by the authors.

Kasegalik Formation

Deposition of the Belcher Group was initiated with the development of a transgressive carbonate platform during rifting of the Superior craton. This early stage is represented by the Kasegalik Formation. The > 1.1 km thick succession consists of supratidal to intertidal facies dominated by very fine-grained dolomicrite to argillaceous dolomicrite packages. The lower contact is not exposed (Jackson 2013), but the formation is suspected to lie unconformably on Archean gneiss of the Superior craton (Mukhopadhyay and Gibb 1981; Roksandic 1987; Corrigan et al. 2021). A zircon U–Pb age of 2018.5 ± 1.0 Ma from a volcanic lapilli tuff found ~150 m above the base of the Kasegalik Formation, in combination with another zircon U–Pb age of 2015.4 ± 1.8 Ma from a volcanic tuff ~100 m below the top of the formation, brackets its depositional timeframe (Hodgskiss et al. 2019b). Detrital zircon grains from two sandstone horizons in the middle part of the Kasegalik Formation (~360 m above the base of the formation) were also analyzed by Hodgskiss et al. (2019b) and are as young as 2120.6 ± 1.5 Ma and 2123.4 ± 1.5 Ma (weighted mean of 5 grains for each sandstone). These provide a maximum depositional age, whereas U–Pb zircon ages from tuff beds are interpreted as depositional ages.

The Kasegalik Formation represents the seaward migration of depositional facies and was informally divided into five gradational units (A–E) by Bell and Jackson (1974). Unit A is the lowermost and consists of thin, red, argillaceous beds (Fig. 4A) and light grey aphanitic (very fine grained) silty dolomicrite beds (Fig. 4B). Red argillaceous beds vary in thickness but are up to 5 m thick and constitute ~20% of the unit (Bell and Jackson 1974). The unit exhibits numerous sedimentary structures indicative of subaerial exposure, such as mud cracks, mud

dykes, and tepees (Ricketts 1979), as well as intervals of brecciated, edgewise-stacked, intraformational conglomerates (Fig. 4C). Horizons of halite casts and sulphate molds associated with the red argillite beds suggest evaporitic intervals (Fig. 4D). Unit B contains similar sedimentary structures but is largely dominated (~60%) by the red argillaceous beds (Bell and Jackson 1974). The combination of sedimentary structures, as well as the presence of crystal molds and casts, led Bell and Jackson (1974) to interpret a sabkha-like environment (a wide tidal salt flat) for the lower two units. Units C and D are mostly composed of light grey to grey stromatolitic dolostone that contain progressively more complicated stromatolite forms up-section. Dominant stromatolitic structures present are domical and lobate forms. Larger structures include low-lying dome-like structures (Fig. 4E). Ricketts (1979) also reported low mounds containing digitate and furcate branching stromatolites (Fig. 4F). Horizons of minor grey and black chert replacement occur throughout the stromatolitic zones but are most common in Unit D. The earliest unambiguous cyanobacterial fossil, *Eontophysalis belcherensis*, was found by Hofmann and Jackson (1969) in this unit. Bedding for both units ranges from laminated to medium-bedded with some beds reaching 1 m thick. Unit E is dominated by pink argillaceous dolostone, in which sulphate molds occur along with red argillite. Dimroth et al. (1970) identified metre-thick tuff beds in the basal part of the unit. Deposition of the Kasegalik Formation ended abruptly with the arrival of the Eskimo Formation basalt flows.

Eskimo Formation

The eruptions forming the Eskimo Formation marked a distinct environmental change for the Belcher Group. The Eskimo Formation ranges from 200 to 1000 m thick and is composed of dominantly massive, aphanitic to porphyritic (Fig. 5C), green–grey basalt flows (Jackson 1960, 2013; Legault 1993) with columnar-jointed interiors and highly vesicular flow tops (Legault et al. 1994). Most of the formation is composed of aphanitic tholeiitic flows, though some plagioclase-phyric flows occur (Fig. 5E). Tuffaceous beds preserving both horizontal and cross-bedded laminae can be observed as well as volcanic breccia (Fig. 5A, B, D). Both the top and bottom contacts of the formation are poorly exposed but are thought to be conformable (Dimroth et al. 1970). Flows vary in thickness across the islands but are defined by an overall thinning towards the south and west (Ricketts 1979), indicating a decrease in volcanic activity in this direction (Dimroth et al. 1970). Although the flows thin, their lateral continuity can be traced for tens of kilometres from north to south (Legault et al. 1994). The formation is interpreted as a series of subaerial continental basalt flows. Locally, intervals of greywacke, sandstone, and conglomerate occur within the formation, which supports the interpretation of subaerial continental flood basalts (Legault et al. 1994). Geochemical investigations by Baragar and Scoates (1987) and Arndt et al. (1987) indicated that the basalt is tholeiitic and shows a negative anomaly of Nb and La (chondrite-normalized). Negative ϵNd (T) values of -7 to -8.7 show crustal contamination of the magmas (Chauvel et al. 1987). Legault et al. (1994) proposed that the formation included basalt with two different parental magma sources, as suggested by higher Zr/Cr ratios in the upper Eskimo Formation compared to its lower part. The consensus of authors who have worked on the Eskimo Formation is that the volcanic flows were extruded during continental rifting.

Fairweather Formation

The Fairweather Formation is divided into a lower member and an upper member, and ranges in thickness from 350 to 600 m across the Belcher Islands. The lower contact with the Eskimo

Formation is poorly exposed but thought to be conformable; the upper contact is conformable and defined as the transition from quartz arenite into dolostone of the McLeary Formation (Ricketts 1979; Fig. 3). The lower member consists of lenticular bodies of ferruginous siltstone, pisolitic dolostone and sandstone (Fig. 6A–C) (Ricketts 1979, 1983). Ricketts (1979) described the basal 160 m of the member as pisolitic dolostone interbedded with thin variegated (red and green) mudstone, siltstone, and immature sandstone (Fig. 6C–D). The upper 150 m of the lower member is dominated by orange-weathered pisolitic dolostone beds that mark the ends of shoaling-upward sequences. Ricketts (1979) observed at least 18 distinct cycles that ranged in thickness from 1 to 30 m, and further divided the cycles into two separate lithological groupings. The basal component of most cycles is composed of herringbone cross-bedded sandstone that contains channels, scour marks, flaser bedding, reactivation surfaces and asymmetrical wave ripples. The tops of individual cycles are dominated by mudstone and siltstone preserving desiccation structures. Individual pods of coarse sandstone and mudstone also occur in the upper parts of cycles. The combination of sedimentary structures and rock types suggests a low-energy mixed tidal flat environment that experienced occasional intervals of higher energy deposition (as shown by the coarse sandstone and mudstone). Paleocurrent determinations by Ricketts (1979) suggest a dominant west-southwest transport direction, indicating that the dominant sediment source was in the east. The second cycle grouping is characterized by the pisolitic dolostone caps, described as displaying asymmetric and composite growth patterns by Ricketts (1979). The asymmetry is due to the effects of gravity preferentially building up the downward facing surface, whereas the composite growth is interpreted to reflect partial dissolution or a change in the carbonate precipitation rate. Thin laminae over the tops of pisolite-rich beds are interpreted as evidence of cyanobacterial mats. Some limited evidence of erosion suggests periodic exposure of the sediments. Ricketts (1979) suggested that the carbonate caps represent caliche beds, implying that each shoaling-upward cycle represents a transition out from an intertidal flat environment to a supratidal environment.

The upper member ranges from 180 to 200 m thick and comprises red and green siltstone and mudstone along with fine-grained sandstone in thick (2–3 m) beds. It is also characterized by a series of cross-cutting channels filled with quartz arenite and sublitharenite. The fine-grained sediments preserve load structures (particularly where they are in close proximity to channels), lenticular bedding and symmetrical ripples (Ricketts 1979). Tabular sandstone units are largely confined to the upper 20 m of the member and contain planar and herringbone cross-bedding, scour marks and large ripples with mud inter-fill (Fig. 6E). Channel lag deposits are also present with some containing grit beds (Fig. 6F). The dominance of finer-grained rock types followed by coarser-grained sandstone units, and the evidence of channels collectively suggest that the upper member was deposited in a tidal flat environment dominated by sand and mud flats (Ricketts 1979).

McLeary Formation

The McLeary Formation conformably overlies the Fairweather Formation and ranges between 250 and 470 m thick. The formation is subdivided into three members, and is dominantly composed of dolomicrite, silty dolomicrite, sandstone and stromatolitic dolostone. The base of the lower member is denoted by repeating cycles of “beachrock” horizons, which were formed by rapid cementation of beach sand at the coastal strandline and mark an upward shoaling cycle (Donaldson and Ricketts 1979). Laterally continuous beds of nodular chert associated with stone rosette horizons are present, as well as intervals of well-laminated, red to maroon siltstone.

Sedimentary structures include abundant trough cross-bedding, possible reactivation surfaces, and scour and fill structures in both dolomicrite and sandstone. Small, finger-like, laterally linked stromatolites are associated with some beachrock beds (Ricketts 1979). Ricketts (1979) interpreted the upward shoaling cycles to represent a transition from a sandy shoreface to a foreshore.

The middle member ranges between 90 and 150 m in thickness, and up to five sandstone and sandy doloarenite beachrock cycles can be identified (Ricketts 1979). Both trough and herringbone cross-bedding can be seen in the sandstone and doloarenite beds (Fig. 7A). As in the lower member, beachrock cycles are also associated with stone rosettes where the stacked tabs were dominantly silty dolomicrite. Ricketts (1979) classified most of the beachrock cycles as grainstone composed dominantly of lithic fragments and possible pisoliths (Fig. 7B). Small digitate stromatolites are also present (Fig. 7C–D) as well as larger domical and columnar non-branching stromatolites near the contact with the upper member (Fig. 7E–F). Intraformational conglomerate composed of silty dolomicrite rip-up clasts and a dolomicrite matrix near the basal part of the member was interpreted by Ricketts (1979) as storm deposits that formed within a supratidal to intertidal environment.

The upper member ranges from 180 to 250 m on Tukarak Island and in Fairweather Sound, but only around 130 m on Flaherty Island near the community of Sanikiluaq. The member marks a change in depositional environment from the lower two members because it is dominated by finely laminated to thinly bedded stromatolitic dolostone units that show progressively more complex stromatolite morphologies up-section. Ricketts (1979) subdivided the member into three gradational zones based on the morphological changes and abundance of these stromatolitic structures. The lower division contains multiple morphologies including parallel, wavy, tufted laminated, stratiform digitate and pisolitic laminate forms (Fig. 7E). The middle division is largely characterized by simple, broad domes ≤ 2 m across with small branching stromatolites occurring at the top. The upper division contains *Conophyton* (Fig. 7G–H), branching and non-branching lobate stromatolites, digitate stromatolites, and branching columnar stromatolites. There are black chert-replaced stromatolites (Fig. 7H) throughout the member but these are mostly found in the upper-middle and upper portions. The upper contact with the Tukarak Formation is denoted by an orange–buff weathered, stromatolitic dolostone unit (Fig. 7I). The increase in abundance and complexity of stromatolite morphologies indicates a completely subaqueous depositional environment such as the subtidal zone.

Tukarak Formation

The Tukarak Formation ranges between 50 and 90 m thick and is an excellent marker unit due to its unique variegated maroon colour and corrugated texture (Fig. 8A–B). Both the top and bottom contacts of the formation are sharp and conformable (Fig. 8C–D) (Ricketts 1979). Jackson (1960, 2013) divided the formation into lower and upper members which Ricketts (1983) used to define the boundary between megacycle 2 and 3 (see later discussion). The lower member is characterized by interbedded grey to pink dolomicrite, olive-green argillite and thinly laminated to wavy bedded silty dolomicrite (Fig. 8B) (Jackson 1960; Ricketts 1979). Immature sandstone beds are also present and contain planar, trough, and herringbone cross-bedding. Lenticular bedding (Fig. 8E–F), wave ripples, and stone rosettes are also found locally within the lower member.

The upper member is characterized by distinctly maroon ferruginous mudstone and buff-coloured dolomicrite interbeds. Reworked angular clasts of silty dolomicrite can be found

between thin (> 1 cm) red argillite beds (Fig. 8G). The preferential weathering of finer grained material (clay, silt, calcite) gives the member its unique corrugated texture (Jackson 2013). Lenticular and flaser bedding along with current ripples, small dewatering structures, and possible desiccation cracks are also preserved (Jackson 2013). Ricketts (1979) also identified stromatolitic mounds in this member. Ricketts and Donaldson (1989) assigned the upper member to a muddy foreshore/shoreface environment that later developed into a muddy platform during deposition of the overlying Mavor Formation.

Mavor Formation

The Mavor Formation is composed primarily of dolomicrite and stromatolitic dolostone and ranges in thickness from 190 to 250 m. The typical bed sequence consists of alternating grey and buff-weathered dolomicrite that appears somewhat nodular or lenticular in places (Fig. 9A). The upper and lower contacts are gradational over a few metres, and both are considered conformable. The Mavor Formation is unique in that it is characterized by very large stromatolite mounds that can be several tens of metres wide, indicating that large platform-building morphologies were dominant.

The deposition of the Mavor Formation represents a seaward transition away from coastal sandy facies to platform reef build-up (Ricketts and Donaldson 1989). The basal part of the formation is dominated by upward-shoaling cycles of dolomicrite to grainstone a few metres thick (Fig. 9B–C) (Ricketts and Donaldson 1989). Sedimentary structures that are commonly associated with shallow subtidal and beach environments, such as stone rosettes, low-angle cross-beds, beach stones, flaser (Fig. 9D), lenticular and wavy bedding, and a variety of microbial mat structures (Donaldson and Ricketts 1979; Ricketts and Donaldson 1989). Evidence of deep burial and carbonate dissolution is also present in the form of stylolites (Fig. 9E). Ricketts and Donaldson (1989) discussed grey thrombolite mounds interbedded with sandstone. They commented on the intermingling of the thrombolite facies with the intertidal sand facies and platform margin facies, which they argued suggests a transitional shallow marine setting. The most striking feature of the Mavor Formation is its stromatolitic mounds that represent reef build-up. While this is typically present as three reef build-ups within the formation, stromatolitic mounds can comprise the entire formation (Ricketts 1979; Ricketts and Donaldson 1981; Sherman 1993). The mounds are dominantly composed of branching digitate and columnar stromatolites, wavy and crinkly microbial laminates (Fig. 9F–H). Mound amplitude and spacing increase up-section but then diminish and transition into thin laminated dolomicrite beds with only rare stromatolites near the top (Ricketts and Donaldson 1989). Ricketts and Donaldson (1989) observed elongation in the stromatolitic mounds that is parallel to inferred paleoslope and transport directions towards the southwest.

Costello Formation

The Costello Formation is characterized by hundreds of metres of rhythmically bedded calcilitite, dololite, dolosiltite, shale–argillite, local calcareous chert and minor intraformational chert, as well as intraformational conglomerate and breccia (Jackson 2013) on top of 40 to 50 m of dark grey to black shale that is poorly exposed (Figs. 10, 11A). Some of these beds are turbiditic (Ricketts 1979). Diabase sills intrude the basal contact of the Costello Formation on western Tukarak Island and along the east limb of northern Kasegalik anticline (Fig. 2C), where there are carving stone occurrences along the contact (see later discussion). The formation ranges between 240 and 370 m thick in total and represents deposition of sediment

along a platform slope. A black to grey to calcareous shale occurs in the basal 20 to 40 m of the unit and is gradational with the underlying Mavor Formation (Ricketts 1979; Sherman 1993; Jackson 2013). Above the basal unit is ~100 m of dominantly buff-coloured dolomicrite which transitions to a maroon dolomicrite that dominates the remainder of the formation (Fig. 10). Horizons of nodular calcite are present throughout the formation and are responsible for the corrugated texture of the rock (Fig. 11B). Bed thickness decreases as clay content increases with stratigraphic height, indicative of a more distal depositional environment (Ricketts and Donaldson 1989). Intraformational conglomerate beds (Fig. 11C), slump folds (Fig. 11D) and turbidite deposits (a–c of the Bouma cycle) are all present in the upper third of the formation. Slump folds identified by Ricketts (1979) indicate a west or southwest sediment transport direction. The culmination of thin interbeds and partial Bouma sequences supports the interpretation of slope deposits by Ricketts (1979).

Laddie Formation

The Laddie Formation is divided into a lower and upper member, with a total thickness between 230 and 250 m. The bottom contact is conformable and gradational with the underlying Costello Formation. The lower member is characterized by brownish-red dolomicrite with nodular calcite lenses (Fig. 12) that first appear in the uppermost beds of the underlying Costello Formation. The upper member is dominated by siltstone and cross-bedded sandstone, and its contact with the lower member is gradational over several metres. Ricketts (1979) and Ricketts and Donaldson (1989) suggested that the Laddie Formation was deposited in deeper waters below the storm weather wave base.

Rowatt Formation

The Rowatt Formation is a 330 m-thick succession of terrigenous clastic sedimentary rocks that grades into carbonate-dominated clastic material in the upper portions of the lower member, and then into distinctive dolomicrite grainstone beds of the upper member (Fig. 13A). The upper member is resistant and forms ridges that are easily mapped. A lower- and upper-member division was proposed by Jackson (1960, 2013) and redefined by Ricketts (1979) to better reflect the change in facies from the Laddie Formation to the Rowatt Formation.

The lower member is broken into three intragradational zones by Ricketts (1979), with the lowermost division consisting of quartz arenite and green mudstone cycles. Sedimentary structures include herringbone cross-bedding, large ripples with smaller ripple mounts, and planar cross-beds (Fig. 13B). The quartz arenite beds are interpreted to be dunes or sand bars (Ricketts 1979). The upper portion of the lower member includes more thinly laminated mudstone and siltstone.

The middle zone continues the thinly bedded mudstone and siltstone association with interbeds of fine-grained sandstone (Ricketts 1979). Lenticular bedding dominates and becomes more prominent with stratigraphic height. Sedimentary structures such as herringbone cross-bedding, starved current ripples and reactivation surfaces indicate tide-dominated environments. Conglomerate layers increase in abundance within the middle zone and are commonly composed of reworked dolomicrite and silty dolomicrite clasts (3–5 cm in size) that are either tabular or sub-rounded (Fig. 13C–D). Ricketts and Donaldson (1981) noted that conglomerate is of two types; either well-sorted channel fills or tabular conglomerate that shows lenticular bedding. The upper zone has a higher proportion of carbonate rock types and contains structures suggesting subaerial exposure (Fig. 13E) (Jackson 2013). The interplay of the three zones led Ricketts

(1979) to interpret the sequence as a landward progression out from the lower to mid tidal flats (zone A), to mid, mid-upper tidal flats (zone B), capped by storm deposits in the mid-upper tidal flat of the lower zone C, and eventually ending in the upper tidal flat nearing the contact with the upper member of the formation.

The transition from lower to upper member within the Rowatt Formation is denoted by a marked visual contrast in colour associated with a change in rock types (Fig. 13F). The upper member is dominated by dolomicrite and grainstone beds typically less than a metre thick (Fig. 13A). The member contains rare white to grey chert horizons in addition to rounded chert fragments within many of the grainstone beds. The unit contains many channels in the upper portion, with the fill dominantly composed of dolomitic sandstone and grainstone. Ricketts (1979) measured trough cross-bedding and found a strong unimodal flow direction towards the west. The upper portion of the member is characterized by a series of upwards-shoaling cycles composed of dolomicrite and sandstone interbedded with brecciated dolomicrite. The upper member only rarely contains stromatolites.

Mukpollo Formation

The Mukpollo Formation is almost entirely composed of mature quartz arenite and ranges between 120 and 160 m thick. It contains straight-crested wave ripples, trough cross-beds and local channel structures filled with quartz arenite (Fig. 14A). Thinly laminated, very fine to fine dolomitic sandstone interbeds (Fig. 14B) separate larger bed sets of alternating light and dark coarse-grained quartz arenite (Fig. 14C). Ricketts (1979) interpreted the Mukpollo Formation to represent an intertidal environment. The maximum depositional age of the Mukpollo Formation as determined by the youngest detrital zircon is 2100 ± 33 Ma (Corrigan et al. 2021), although its true depositional age is likely much younger. Paleocurrent data from ripples, megaripples, and planar cross-bedding in the Mukpollo Formation indicate paleocurrent flow towards the northeast and southeast (Ricketts 1979).

Kipalu Formation

The Kipalu Formation ranges between 65 and 130 m in thickness and has a sharp lower contact with the underlying Mukpollo Formation, considered to be conformable (Ricketts 1979; Jackson 2013). The upper contact is with the Flaherty Formation but is nearly everywhere obscured by an intrusive gabbro sill (the Haig intrusions; see later discussions), but a few thin tuff beds occur in the upper Kipalu Formation, suggesting the start of active volcanism prior to the first Flaherty Formation lava flow. The Haig intrusions can also occur in the middle of the unit. This formation was originally named the Keepaloo Formation by Moore (1918), who was also the first to postulate possible algal microfossils in this unit, regarded by Hofmann (1971) as pseudo-fossils. The formation is dominated by variably iron-rich argillite beds and lenses and nodular horizons of granular and oolitic jasper (Fig. 15A–E), associated with minor micrite. Ricketts (1979) divided the formation into six sub-units or zones based on three sections located on Innetalling and Tukarak islands. Twelve other measured outcrop sections represented in Jackson (2013) on Flaherty and Kugong islands show a high variability in the thickness and occurrence of various facies. According to the sections of Ricketts (1979), the lower three zones consist of highly fissile grey–green micrite and red argillite. Beds range from < 1 mm to 80 mm thick. Lenses of granular jasper occur near the base of the lower zone. Sedimentary structures are rare but small-scale trough cross-bedding is present in minor sandstone layers (Fig. 15F). Zones 2 to 4 record a transition from well-bedded argillite and micrite to similar rocks with more wavy or lenticular

bedding. The rocks become noticeably less fissile and bedded granular iron formation (GIF) units become thicker (~30 cm) up-section (Ricketts 1979). Zones 5 and 6 represent a transition from the GIF units to dominantly thinly bedded to laminated red-brown argillite. The dominantly laminated sedimentary rocks of the Kipalu Formation suggest a low energy depositional environment, where sediment fallout was the primary accumulation mechanism, though cross-bedding exists. Ricketts (1979) suggested that the lack of bottom water current features implies deposition below active wave base or within a protected basin. Ricketts (1979) suggested the Kipalu Formation was deposited in a protected basin setting formed through sandbar development during the deposition of the Mukpollo Formation. Although undated, the Kipalu Formation is likely correlative with other ca. 1.87 Ga circum-Superior granular iron formations. For example, the Biwabik iron formation of the Animikie Group in the Lake Superior region of the USA and Canada is constrained between 1874 ± 9 Ma and 1878 ± 1.3 Ma (Fralick et al. 2002; Schnieder et al. 2002). The minimum age of the Kipalu Formation is well constrained at 1870.3 ± 0.7 Ma (Hamilton et al. 2009) by intrusion of the Haig gabbro.

Flaherty Formation

The Flaherty Formation is largely composed of pillowed and massive basalt and minor volcanoclastic rocks (Fig. 16). The formation varies greatly in thickness (500 to 1600 m) across the Belcher Islands but is thickest on the western edge of the islands (Ricketts et al. 1982). Ricketts et al. (1982) also observed that minor sedimentary rocks, including turbidites, are more abundant towards the east, which supports the interpretation of a western source for the volcanism (also suggested by Dimroth et al. 1970), and a deepening of the basin to the east. Paleocurrent data from paleoflow azimuths suggest volcanic flows were predominantly from the west (Ricketts et al. 1982). Generally, the Flaherty volcanic package thins eastwards from ~2000 m in the west to ~300 m in the east on Tukarak Island (Ricketts et al. 1982).

Leggett (1974) suggested that Flaherty Formation volcanism occurred in three stages based on the proportion of pillowed flows to volcanoclastic rocks; an initial weakly explosive stage was followed by an effusive stage defined by extensive and thick flows, which was followed by a combined effusive and explosive phase defined by a mixture of flows and tuffs. Ricketts et al. (1982) argued that this sequence proposed by Leggett (1974) is not found everywhere on the islands and so may have only local significance. Instead, Ricketts et al. (1982) proposed that the Flaherty Formation began with a submarine effusive phase, followed by an explosive phase, and finished with a second submarine effusive phase. This is almost the exact opposite of the earlier interpretation by Leggett (1974) and likely attests to the intrinsic complexity of volcanic environments in three dimensions. Ciborowski et al. (2017) studied the major and trace element geochemistry and Sm–Nd isotopes of the Flaherty Formation from both the Sleeper and Belcher islands. They showed the Flaherty Formation to consist of alkali basalt, enriched in LREE relative to HREE, with positive ϵ_{Nd} and ϵ_{Hf} values that demonstrate juvenile magmas from a depleted mantle source. Ciborowski et al. (2017) suggested these characteristics are consistent with plume-related magmas that are part of the Circum-Superior large igneous province event along with other volcanic successions along the Superior craton margin.

While the proportion of volcanoclastic material has similarities to oceanic island arcs (Ricketts 1981), its uniform geochemistry is inconsistent with the typical magma evolution of a volcanic arc. Jackson (in Dimroth et al. 1970) suggested the volcanic flows emanated from a north–south fault in a rift zone west of the Belcher Islands; other authors supported the rift interpretation from either geochemical or regional considerations (Baragar and Scoates 1981, 1987; Ricketts and

Donaldson 1981; Chauvel et al. 1987; Chandler 1988; Legault et al. 1994; Baragar 2007). Jackson (2013) ascribed the Flaherty Formation to foredeep development in the Nastapoka Arc associated with syn-collisional extension in the Trans-Hudson orogen (Hoffman 1987, 1990; Hynes 1991); syn-collisional magmatism is often mistakenly attributed to the initial rift stages of a Wilson cycle (Bradley 2008), which might explain some of the discrepancies in basin tectonic interpretation.

There are no direct geochronological data from the Flaherty Formation flows. Its age is constrained near its base to be older than ca. 1870 Ma, based on the data from the Haig intrusions (Hamilton et al. 2009), and its upper parts must be older than 1854.2 ± 1.6 Ma, based on the age of a tuffaceous shale found 5 m above the Flaherty-Omarolluk formational contact (Hodgskiss et al. 2019b; see below). In some treatments of the Belcher Group, the age of the Haig intrusions is assumed to also represent the age of the Flaherty Formation (e.g. Jackson 2013).

Omarolluk Formation

The Omarolluk Formation overlies the volcanic rocks of Flaherty Formation, possibly in disconformable contact (Ricketts 1979). It is characterized by well-bedded feldspathic greywacke and shale (Fig. 17) and is the thickest formation within the Belcher Group (> 2000 to 3100 m) (Ricketts 1979, 1981; Jackson 1960, 2013). The base of the Omarolluk Formation is precisely dated at 1854.2 ± 1.6 Ma by U–Pb analysis of zircon from a tuffaceous shale in the lowest five metres of the unit (Hodgskiss et al. 2019b). The formation is subdivided into a lower and upper member and is interpreted to represent a series of deep water turbidite successions (Jackson 1960; Ricketts 1979, 1981) that formed in response to a shift in tectonic environment in response to accretionary and collisional tectonics associated with the Trans-Hudson orogen. Six facies were defined by Ricketts (1981), most of which relate to turbidite facies. The lowermost 5–20 m of the formation consists of either black pyritic shale with a few cherty lenses, interpreted to reflect deposition in a highly reducing, deep water environment producing very fine-grained sandstone, lithic greywacke, or tuffaceous shale (Ricketts 1981; Jackson 2013). The turbidite facies division accounts for approximately 75% of the formation (Ricketts 1981). Of these turbidite facies, most beds preserve the $T_a - T_d$ of the Bouma sequence entirely, but partial sequences are also present (Fig. 17A). Post-depositional structures, such as dewatering pillars and calcite concretions (Fig. 17B), are common throughout the facies (Ricketts 1981). A third facies is characterized by composite beds, interpreted to represent either erosion of finer grained sediments by later turbidite flows, or the inability of finer grained sediments to gain traction and accumulate (Ricketts 1981). The fourth facies is represented by thin-bedded siltstone and shale, interpreted as the T_c and T_d divisions from diluted turbidity flows (Fig. 17C). Ricketts (1981) discussed the possibility that these represent the most distal edge of the turbidite flow or even overbank flow within a channel system. The fifth facies includes channel lag deposits (Fig. 17D) and the sixth facies division relates to rocks that represent the upper contact transition from deeper water turbidites to shallow water and fluvial deposits of the overlying Loaf Formation. All six facies proposed by Ricketts (1979, 1981) are present within the lower member, whereas the upper member is largely composed of the composite-bedded facies and the transitional facies. Post-depositional structures such as dewatering pillars are present within the upper member as well as large scale (> 1 m) slump folds (Fig. 17E). These facies were used to reconstruct the depositional environment represented by the outer and middle portions of a submarine fan that shallows upwards into shallow marine, fluvial and terrestrial sedimentation associated with the Loaf Formation (Ricketts 1981).

Paleocurrents from flute casts, groove casts, parting lineations and current ripples in the Omarolluk Formation indicate bimodal paleocurrent directions to the northwest and southeast, but dominantly indicate a paleocurrent toward the southeast (Ricketts 1981). The Omarolluk Formation incorporates mafic volcanic material and cratonic quartzo-feldspathic material (Jackson 2013). Jackson (2013) interpreted the main sources of the volcanic detritus to be derived from the Flaherty Formation and/or the central Hudson Bay hinterland, whereas Corrigan et al. (2021) inferred that the dominant cratonic source for the Omarolluk Formation is from the Sugluk block as it collided with the Ungava promontory of the Superior craton. Provenance analysis by coupled zircon U–Pb and Hf isotopes is part of our ongoing research and will hopefully provide insight into tectonic events surrounding the Superior craton during the later stages of Manikewan Ocean closure.

Loaf Formation

The Loaf Formation overlies the Omarolluk Formation and is the uppermost stratigraphic unit in the Belcher Group. Although the Omarolluk–Loaf contact is not exposed on the islands, it is assumed to be gradational as the Omarolluk Formation shows a shallowing-upwards progression towards its top (Ricketts 1979; Jackson 2013). The Loaf Formation is 675 m thick and is subdivided into upper and lower members (Ricketts 1979, 1981). The lower member is dominated by very fine to fine-grained feldspathic greywacke in thinly laminated beds (Fig. 18A). Unidirectional ripple structures can be observed near the base of the formation (Fig. 18B) and trough cross-bedding can be seen closer to the upper member contact. The upper member is dominated by pinkish arkose sandstone, conglomerate, and mudstone-siltstone facies (Fig. 18C–E). Sedimentary structures include large planar and trough cross-beds (Fig. 18F), desiccation structures, and ball and load structures, all of which are characteristic of fluvial environments. Overall, the Loaf Formation contains some sedimentary fragments, and very few volcanic fragments, which decrease up-stratigraphy. Paleocurrents indicate predominantly southeast flow indicated by trough cross-beds and easterly transport indicated by low-angle cross-beds (Jackson 2013). Data from U–Pb detrital zircon geochronology indicate a maximum depositional age of ca. 1835 Ma. Corrigan et al. (2021) obtained a youngest detrital zircon age of 1835 ± 7 Ma for the uppermost Loaf Formation, consistent with unpublished data by McDonald and Partin that determined a weighted mean of 1838 ± 16 Ma for three youngest detrital zircon grains analyzed in the lower Loaf Formation. Based on paleocurrent directions, it was suggested by Jackson (2013) that detritus was supplied in large part from the Central Hudson Bay hinterland (Roksandic 1987; Hoffman 1990), or from a source northwest of the present-day Belcher Islands (Ricketts and Donaldson 1981). By contrast, Corrigan et al. (2021) proposed that detritus is derived from the Sugluk block, which would imply a south or southwesterly flow.

Igneous Rocks

Haig Intrusions

The Haig intrusions are aphyric to finely plagioclase-phyric tholeiitic gabbro dykes and sills that occur throughout the Belcher Islands (Jackson 1960, 2013). Similar intrusions occur on the Sleeper Islands, intruding volcanic rocks included with the Flaherty Formation (Baragar 2007). On the Belcher Islands, they are most abundant as a sill at the contact between the Kipalu and Flaherty formations (Fig. 3), but also intrude the entire lower and middle Belcher Group, including the Kasegalik and Eskimo formations, as sills or low angle dykes. These relationships

are shown in partly schematic form in the cross-section in Figure 2. Gabbro sills are not recorded in formations above the Flaherty Formation. The intrusions vary in thickness (up to 280 m thick) but are typically 10 to 20 m thick and locally contain inclusions of Belcher Group units (e.g. Laddie Formation; Jackson 2013). Contact aureoles adjacent to the sills were only observed in the Kipalu and Costello formations (Jackson 2013). The margins of at least some of these intrusions were recrystallized and altered via hydrothermal fluid interaction with country rocks, and zones of this type within the Costello Formation represent carving stone resources (e.g. Steenkamp et al. 2017). The mineralogy reflects recrystallization via low-grade metamorphism and metasomatism rather than primary igneous mineralogy, and includes labradorite feldspar, clinopyroxene, actinolite, chlorite, augite, hornblende with trace minerals comprising ilmenite, magnetite, pyrite and chalcopyrite (Jackson 2013). Some sills display a relict primary subophitic or ophitic texture (Laarman 2004; Jackson 2013). Based on field relationships and mineralogical characteristics, Dimroth et al. 1970 considered the Haig intrusions to be related to Flaherty volcanism, and this was later supported by geochemical comparisons with the Eskimo and Flaherty formations (Legault et al. 1994). Legault et al. (1994) also showed that paleomagnetic pole positions for the Haig intrusions and the Flaherty Formation volcanic rocks coincide, supporting interpretations by Dimroth et al. (1970). This interpretation is also consistent with the stratigraphic distribution of the Haig intrusions, which implies that they could represent feeder systems and subvolcanic components related to mafic volcanic rocks of the Flaherty Formation.

Two precise U–Pb baddeleyite geochronological analyses by Hamilton et al. (2009) yielded identical ages of ca. 1870 Ma for two Haig sills; one intruding the Flaherty Formation on the Sleeper Islands (1870.1 ± 1.1 Ma) and another intruding the Eskimo Formation on the Belcher Islands (1870.3 ± 0.7 Ma). The age of the Haig intrusions is much younger than ages from earlier sedimentary rocks of the Kasegalik and Eskimo formations in the lowest part of the Belcher Group. Careful and detailed field and petrographic documentation by Jackson (2013) was important in confidently assigning the sills that intrude the Eskimo Formation as lithological equivalents of those that intrude the Flaherty Formation.

Geochronological Constraints of the Belcher Group

In the preceding section, important age constraints from the Belcher Group were noted in the context of specific stratigraphic units and these are indicated in Figure 3. However, these are not the only geochronological data, and several problems remain for future attention.

Early attempts at dating used whole rock K–Ar, Rb–Sr, and Pb–Pb geochronology (Wanless et al. 1965, 1967, 1968 Fryer 1972; Dimroth et al. 1970; Todt et al. 1984; Arndt and Todt 1994) but these yielded imprecise results. Nevertheless, this work was important in establishing that the Belcher Group is Paleoproterozoic and confirming potential geological correlations with other parts of the Canadian Shield.

The base of the succession is dated by zircon U–Pb ages from two tuffaceous horizons (2018.5 ± 1.0 Ma and 2015.4 ± 1.8 Ma; Hodgskiss et al. 2019b) located near the base and top of the Kasegalik Formation and provide depositional ages for the lowest rocks in the Belcher Group. These ages are consistent with detrital zircon data from the formation, which show that it must be younger than ca. 2121 Ma (Hodgskiss et al. 2019b). A Pb–Pb age of 1960 ± 60 Ma (Todt et al. 1984) is within error of the ca. 2015 tuff age from the base of the Eskimo Formation, however it is imprecise and unlikely to be accurate considering that only a short timeframe is needed to extrude the basaltic pile represented by the Eskimo Formation. The next unit with an

age constraint is the Mukpollo Formation with a maximum depositional age of 2100 ± 33 Ma (Corrigan et al. 2021).

A U–Pb baddeleyite age (1870.3 ± 0.7 Ma; Hamilton et al. 2009) from plagioclase-phyric gabbro (Haig sills) provides a minimum age constraint on the pre-Flaherty Belcher Group (assuming that all the gabbroic intrusions are actually of that age), since the Haig sills intrude all formations up to the lower Flaherty Formation (Jackson 2013). While there are no geochronological data from the volcanic flows of the Flaherty Formation, which was proposed by earlier studies to be the extrusive equivalent of the Haig sills, a tuff at the base of the overlying Omarolluk Formation with an age of 1854.2 ± 1.6 Ma provides a reliable minimum age constraint on the volcanism. Documenting the timing and duration of this major volcanic episode is an important objective for further research.

The middle and upper formations of the Belcher Group are constrained by U–Pb detrital zircon data and U–Pb igneous zircon from a tuff (Hodgskiss et al. 2019b; Corrigan et al. 2021; McDonald and Partin, unpublished data). The zircon U–Pb age obtained from a tuffaceous shale located five metres above the contact of the Flaherty Formation and the Omarolluk Formation (1854.2 ± 1.6 Ma; Hodgskiss et al. 2019b) constrains the end of Flaherty Formation volcanism but indicates that the uppermost two formations in the Belcher Group were deposited about 160 million years later than those at the base of the Belcher Group. This provides a maximum depositional age constraint on foreland basin development associated with the later stages in the closure of the Manikewan Ocean and the ensuing collision of the Superior craton with other Archean blocks. The maximum depositional age for the uppermost Loaf Formation of 1835 ± 7 Ma (Corrigan et al. 2021) extends the total time period represented by the Belcher Group to > 183 million years. It is hard to discount the possibility that there may be a significant time break within the sedimentary rocks conventionally grouped together as the Belcher Group. This has implications for other studies that use this record to try and understand aspects of ocean and atmosphere evolution within the Paleoproterozoic.

Depositional Evolution of the Belcher Group

Deposition of the Belcher Group was initiated sometime before ca. 2019 Ma and continued for nearly 185 million years, assuming that it is continuous. Broadly, deposition can be broken into several depositional stages (Fig. 3). The initial transgressive marine sedimentation stage is represented by the Kasegalik Formation. This is an upwards-deepening sequence of supratidal to shallow subtidal carbonate rocks that contains evidence of evaporite formation, implying periods of extended subaerial exposure (Ricketts 1979). This environment persisted for some 3 million years, on the basis of recent geochronology (Hodgskiss et al. 2019b; see above). The second stage of deposition involved the eruption of the tholeiitic basalt flows of the Eskimo Formation, which are interpreted to represent continental flood basalt associated with rifting. Pillowed flows are rare, and massive columnar jointed basalt associated with terrestrial sedimentary rocks indicate subaerial conditions.

A second, much longer period of transgressive carbonate platform deposition began following the Eskimo Formation volcanism. This phase was subdivided into three “megacycles” by Ricketts and Donaldson (1981). The first of the three megacycles is characterized by upwards-shoaling cycles. Coarse grit beds forming lag deposits in the upper member of the Fairweather Formation imply tidal channels, which suggests that there was some subaerial exposure during the first megacycle. Evidence of beachrock deposits within the lower McLeary Formation suggests a short-lived period of shoreline progradation at the onset of the second megacycle, but

the dominance of deeper intertidal and shallow subtidal dolomitic facies and the appearance of stromatolites within the middle and upper members of the McLeary Formation indicate a return to a transgressive carbonate platform. Following deposition of the McLeary Formation and the lower Tukarak Formation, the prograding stromatolitic reefs complexes of the Mavor Formation were developed, also with beachrock deposits, and these are capped by grey to black shale overlain by interbedded dolomicrite units of the Costello Formation. Intraformational conglomerate, slump folds and incomplete Bouma sequences suggest a platform–slope margin setting where sediment could be subjected to turbiditic reworking (Ricketts 1979). The overlying Laddie Formation is the final stage of sedimentation in the second megacycle and represents a deep-water environment.

The third megacycle begins with a distinct change in depositional environment from the deeper water setting of the Laddie Formation into the dominantly shallow subtidal to intertidal environment of the Rowatt Formation. The lower member of the Rowatt Formation includes many shallowing-up cycles composed of quartz arenite and mudstone, and herringbone cross laminations imply a strong tidal influence. An overall increase of lenticular bedding up section and evidence of channels suggest a transition into a tidal flat environment. Metre-scale beds of dolomicrite and grainstone in higher parts of the formation represent shoaling-up cycles and stromatolitic horizons appear. Ricketts (1979) interpreted the upper part of the Rowatt Formation to record carbonate platform buildup bounded by an intertidal platform on its seaward side. The overlying Mukpollo Formation contains mature quartz sandstone interpreted to represent tidal sand bars, and the argillite and granular iron formation of the Kipalu Formation were interpreted to reflect the development of an associated barred basin protected by a system of carbonate buildups and offshore sand bars, potentially analogous to the barrier island–lagoon complex in modern day Gulf of Mexico (Ricketts 1979).

The final phase of sedimentation, following the lengthy volcanic interval represented by the Flaherty Formation, involved the development of a prograding submarine turbidite fan (Omarolluk Formation) interpreted to represent flysch deposits, followed by shallow-water sedimentary rocks interpreted to represent molasse deposits (Loaf Formation) (Ricketts 1981). The Omarolluk Formation contains at least 3,100 m of overlapping turbidite sequences interpreted to represent deeper marine sedimentation (Jackson 2013). The overlying Loaf Formation contains at least 675 m of fine- to medium-grained arkose and arkosic sandstone beds with cross-bedding and intraformational conglomerate interpreted to represent shallow marine, fluvial, and terrestrial sedimentation (Jackson 2013). Intraformational conglomerate of the upper member contains much larger clasts and led Ricketts and Donaldson (1981) to interpret some of these rocks as products of braided rivers. Overall, the transition between the Omarolluk and Loaf formations documents a shallowing-upwards succession.

Structural Geology and Metamorphism of the Belcher Group

Although the sedimentary rocks of the Belcher Group are remarkably well preserved, they experienced deformation, mostly folding, as a distal part of a thin- to thick-skinned fold and thrust belt (Jackson 2013; Corrigan et al. 2021). The tight to locally isoclinal folding is visually obvious in the very shapes of the islands, which define several regional-scale anticlines and synclines, including the Tukarak anticline and the north-plunging Omarolluk syncline (Fig. 2). The Tukarak anticline is an open fold, whereas the Omarolluk syncline is more tightly folded. Many other smaller fold structures are also recognized, and there is a weakly developed crenulation cleavage associated with regional folds (Jackson 2013). Faults are a relatively minor

structural feature on the Belcher Islands. The few major faults are steeply dipping and interpreted to post-date folding (Jackson 2013). Small local thrust faults are observed, including one that displaces a Haig sill on Mavor Island. There is little evidence of structural repetition of stratigraphic units. Jackson (2013) noted that most contacts are gradational between formations and members and that the lavas of the Flaherty and Eskimo Formations are associated with tuff horizons in both the underlying and overlying sedimentary rocks, reinforcing this concept. Dimroth et al. (1970) postulated that a décollement separates the Belcher Group from the underlying basement rocks, which would have occurred early in its structural history. Late brittle deformation is indicated by faults that contain slickenlines defined by calcite or actinolite growth (Steenkamp et al. 2016) and by calcite–quartz veins that primarily occur within volcanic units (Eskimo and Flaherty formations) and in the Omarolluk Formation (Jackson 2013).

A mineral assemblage that includes chlorite, titanite, sericite, prehnite and pumpellyite found in volcanic rocks of the Eskimo and Flaherty formations suggests that the Belcher Group experienced only low-grade regional metamorphism at prehnite-pumpellyite to lower greenschist facies (Leggett 1974; Jackson 2013). A low degree of crystallinity of kerogen (i.e. disordered organic matter) in McLeary Formation stromatolites indicates temperatures between about 241 and 358°C (Gabriel et al. 2021), which matches those inferred on the basis of metamorphic mineral assemblages. Contact interaction (metamorphism and metasomatism) associated with the Haig intrusions resulted in decarbonization of dolostone and calcareous shale units (notably the Costello Formation) and formation of talc–calcite soapstone along gabbro unit margins. Many carving stone resources are related to these processes (e.g. Laarman 2004; Steenkamp et al. 2016).

Economic and Cultural Geological Resources

Iron Ore

The Belcher Islands have mineral potential in the form of iron ore from the Kipalu Formation, which is considered to be a Superior-type iron formation. This potential was recognized very early (Flaherty 1918) and was the reason for most geological research prior to the late 1950s. Early work in the 1950s by the Belcher Mining Corporation Ltd. found deposits grading 27% Fe on Innetalling Island, located approximately 50 km southeast of Haig Inlet (summarized by Jackson 1960). The general conclusion from 20th century exploration was that deposits were too small, too remote, and too low in grade to be of commercial interest. There was little or no exploration for the remainder of the 20th century, but interest resumed in 2011 when iron ore prices were high and demand growth was anticipated from the Chinese economy. Canadian Orebodies Inc. began a drill program in the area of Haig Inlet, south of Sanikiluaq. The target is the Kipalu Formation, which also occurs in many other locations across the islands.

Wahl (2012) summarized the results of the most recent (2011) drill program, which mostly targeted two deposits known as Haig Inlet North and Haig Inlet South. The indicated resources at Haig Inlet North are 230 million tonnes (at 35% Fe); inferred resources at both Haig Inlet North and Haig Inlet South represent an additional 289 million tonnes at slightly lower grades. Although the company expressed great optimism about the prospects for development at the time, no preliminary economic assessment was completed, and no exploration work was completed since 2012. The grades of mineralization at Haig Inlet are relatively low, and material would likely require on-site beneficiation; the establishment of such infrastructure on remote islands in Hudson Bay could present challenges. Unlike other iron formations in sedimentary

sequences equivalent to the Belcher Group, supergene iron enrichment through deep weathering is not reported on the Belcher Islands.

Carving Stone

Carving stone in Nunavut is considered a “long-term commodity” and the quarries on Belcher Islands are estimated to provide at least four decades of production (Beauregard and Ell 2015). Nunavut’s carving stone commodities have recently been categorized by the Nunavut Carving Stone Deposit Evaluation Program, led by the Government of Nunavut in collaboration with the Canada–Nunavut Geoscience Office and local community carvers. Having both locally and regionally available quality carving stone is important to the local communities; carvings can sell for hundreds of dollars and serve to pass traditional Inuit knowledge between generations.

The Belcher Islands are well-endowed with carving stone deposits (Fig. 19), which can be either green or black in colour, and consist primarily of talc. A recent calculation estimates 30,000 tonnes of artisan marble reserves occur at Sanikiluaq’s main community quarry, the Qullisajaniavvik quarry on Tukarak Island (Beauregard and Ell 2015). This is located south of the old Hudson’s Bay Company outpost on Tukarak Island (Fig. 19). The Qullisajaniavvik quarry represents an ideal setting to observe the geological processes responsible for generating the carving stone, including contact metamorphism and metasomatism where the Haig sills intrude into the Costello Formation. Other carving stone locations include two quarries on Tukarak Island (Qullisajaniavvik, Aqituniavvik), Salty Bill Hill, and Kasegalik Lake (locations in Beauregard and Ell 2015). Laarman (2004) suggested the location of the main quarry is due to the preservation of soapstone textures within a strain shadow in the inner limb of the Tukarak anticline; elsewhere this texture has been largely overprinted by regional deformation. At the Qullisajaniavvik quarry, artisan marble is locally referred to as ‘argillite’ and is a “competent, soft to medium-soft rock” (Beauregard and Ell 2015) that can be carved by hand. Timlick et al. (2017) used the Mohs hardness scale to quantify the softness of the stone. They note that the hardness of quarried carving stone ranges in hardness from “too soft to carve with power tools” (Mohs hardness of < 2), to “being able to hold a fine detailed polish” (Mohs hardness of ~2.5) where it is directly in contact with the Haig sill. This quarry has been producing since the 1970s. Carving stone from Qullisajaniavvik quarry is highly regarded due to its character, which includes its ability to hold fine detail, and the ability to achieve a smooth polish on the finished product (Timlick et al. 2017). Two smaller inland quarries at Salty Bill Hill on Tukarak Island host 100 tonnes each of good quality “medium-soft” artisan marble (Beauregard and Ell 2015). Kipalu Inlet (Fig. 2C), on the coast of the southern Belcher Islands, contains reserves around 100 tonnes (Beauregard and Ell 2015). The artisan marble found on the Belcher Islands was formed by the intrusion of gabbro sills into dolostone units; quarries are concentrated on the east side of the Belcher Islands due to the occurrence of the Haig sills there, and the presence of an anticline structure that exposes the contact between dolostone and gabbro sills. Carving stone deposits are interpreted to have formed within thermal aureoles of the sills via hydrated talc–calcite growth in concert with decarbonation of dolomite (Laarman 2004). The source of the fluids causing this hydration is somewhat debated in Laarman (2004). One interpretation is that the Haig gabbro sills intruded into wet sedimentary units and the source of hydration was essentially sedimentary pore fluid or modified seawater. However, Laarman (2004) demonstrated a late introduction of hydrothermal fluids that postdated the crystallization of the intrusions. Thus, the occurrence of soapstone within the Costello Formation may involve hydrothermal or magmatic fluids associated with the intrusion (Laarman 2004). The process of “autohydration”, whereby new

minerals form in an igneous rock from the reaction of water with existing magmatic minerals, is thought to explain the mineralogical changes including alteration of pyroxene, replacement of plagioclase by calcite, zoisite and chlorite, formation of epidote and alteration of ilmenite (Laarman 2004). Magmatic fluids and heat from the gabbro sill caused decarbonization of dolostone and argillaceous dolostone units and formed talc–calcite soapstone adjacent to gabbro contacts. The presence of interbedded argillaceous and dolomitic rock types was a key factor in providing the elements necessary to create these unusual, altered rocks in contact regions.

The rock type found at the Qullisajaniavvik quarry is a dolomitic talc carbonate, whereas the original rock (protolith) is an argillaceous dolostone of the Costello Formation (Timlick et al. 2017). The mineral assemblage of the artisan marble is dolomite–calcite–talc–chlorite ± quartz and it can be divided into two distinct varieties based on degree of alteration (Timlick et al. 2017). All the quarries on Tukarak Island involve the middle member of the Costello Formation and are sited where it is intruded by Haig sills (Jackson 2013); this relationship is a good predictor of future potential quarry sites (Steenkamp et al. 2016). In this area, the thickness of the Haig intrusion correlates with the thickness of the contact metamorphic and metasomatic aureoles, which also tend to be thicker stratigraphically beneath the sill than above it (Steenkamp et al. 2016).

Other Commodities

Other commodities noted by various studies are minor in nature. Mafic igneous rocks that are broadly equivalent in age to those of the Flaherty Formation and Haig sills elsewhere in Canada host important magmatic Ni–Cu sulphide deposits, such as at Thompson, Manitoba. However, very little sulphide mineralization occurs on the Belcher Islands, apart from some minor copper occurrences associated with gabbro sills and minor pyrite and/or pyrrhotite in the Flaherty Formation (Jackson 2013).

UNIQUE GEOLOGICAL FEATURES OF THE BELCHER ISLANDS

Exceptional Preservation

Many Paleoproterozoic sedimentary rocks are transformed by later deformation, metamorphism, and alteration to the extent that many physical and/or chemical characteristics that recorded their deposition are lost. The Belcher Group was not as deeply buried as some contemporaneous sedimentary–volcanic packages, because it was deposited on continental crust of the Superior craton that was also located within an embayment that shielded it from much of the deformation that other areas in the Trans-Hudson orogen experienced (Hoffman 1985). However, it did not escape deformation entirely, as evidenced by the fold structures that so clearly define the shapes of the islands (Fig. 2).

Despite obvious regional and local tectonic structures that resulted from the Trans-Hudson orogen, the Belcher Group preserves many primary structures including cross-bedding, dewatering structures, desiccation cracks and a wide range of other depositional features. The early diagenetic silicification of dolostone units (Hofmann 1976) was an important factor that contributed to the preservation of cyanobacteria microfossils (Fig. 20). The Belcher Group is thus an unusual example of well-preserved Proterozoic sedimentary and volcanic rocks that may yet yield other examples of fossil microbes in the geological record.

Unique Timing of Deposition in the Context of the Geochemical Evolution of the Great Oxidation Event

The Paleoproterozoic Earth experienced fundamental changes related to its atmosphere and oceans. These included significant accumulation of atmospheric O₂, leading to oxidative continental weathering that delivered crucial elements to the oceans, where they were utilized as nutrients, promoting greater primary productivity and organic carbon production. The deposition of the Belcher Group began ca. 2.15 Ma, after the so-called *Great Oxidation Event* (Fig. 21). The Great Oxidation Event began ca. 2.3 Ga and saw oxygen rise to ~1–10% of present-day levels; the chemistry of seawater also changed dramatically (e.g. Lyons et al. 2021). Two other important events occurred after the Great Oxidation Event. The ca. 2.2 to 2.05 Ga Lomagundi–Jatuli Event records large-scale burial of organic carbon and a continued influx of atmospheric O₂. The Lomagundi–Jatuli Event is defined by the largest positive carbon-isotope excursion in the geological record, which illustrates massive burial of organic material that was relatively enriched in isotopically light carbon. This influx of O₂ was followed by a dramatic decline in atmospheric and oceanic O₂ levels ca. 1.9 Ga (Partin 2023). It is now thought that early atmospheric oxygen levels oscillated considerably (Poulton et al. 2021) and might have been at their highest later than originally thought, at about 2.2 Ga (Hodgskiss and Sperling 2022). Given the nearly 200-million-year timeframe in which the Belcher Group was deposited, it is likely that its lower formations were deposited under higher O₂ conditions than the upper formations. The Belcher Group is thus an important focus for research aimed at understanding the early evolution of the atmosphere and the oceans (e.g. McDonald et al. 2022). In the following section we review some studies that have improved understanding the geochemical record contained in the Belcher Group.

Carbon isotopes are widely used in studies of the composition of the ancient oceans. Carbon isotopes are largely presented in two ways, either as $\delta^{13}\text{C}_{\text{org}}$ or as $\delta^{13}\text{C}_{\text{carb}}$ values, both terms representing the ratio of ¹³C versus ¹²C within either the organic carbon fraction or the carbonate-associated carbon fraction. $\delta^{13}\text{C}$ values, expressed in parts per mil, with respect to a standard, indicate the relative abundance of ¹³C, with higher values indicating greater relative amounts of the heavier isotope. Prior to deposition of the Belcher Group, and following the Great Oxidation Event, $\delta^{13}\text{C}_{\text{carb}}$ values were high, reaching values between +5 and +15‰ (Hodgskiss et al. 2019a) during the ca. 2.2 to 2.06 Ga Lomagundi–Jatuli Event (Karhu and Holland 1996). Hodgskiss et al. (2019a) measured $\delta^{13}\text{C}_{\text{carb}}$ on samples across all Belcher Group carbonate-bearing formations. The values indicate typical marine conditions with no anomalously high $\delta^{13}\text{C}_{\text{carb}}$ values, suggesting that the Belcher Group postdates the Lomagundi–Jatuli Event, which is consistent with known age constraints. Additionally, Gabriel et al. (2021) analyzed the total organic carbon and carbon isotope ratios for both organic ($\delta^{13}\text{C}_{\text{org}}$) and carbonate ($\delta^{13}\text{C}_{\text{carb}}$) materials in the McLeary Formation stromatolites. The McLeary Formation stromatolites contain relatively low total organic carbon (between 0.06 and 0.31 wt.%), an average $\delta^{13}\text{C}_{\text{org}}$ of $-26.4 \pm 2.3\text{‰}$ and average $\delta^{13}\text{C}_{\text{carb}}$ values around 0‰. The isotopic fractionation between bulk organic and carbonate fractions is consistent with photoautotrophic carbon fixation, indicating oxygenic photosynthesis. This is significant because it supports the interpretation by Hofmann and Jackson (1969) that the microfossils in the same unit represent photosynthetic cyanobacteria. Other geochemistry, including rare earth element patterns, especially Ce/Ce*, show that the Belcher Group was deposited under typical marine conditions (Hodgskiss et al. 2021). The combination of its depositional setting in an open-ocean (non-restricted) basin and formation in a critical time

interval makes the Belcher Group a potential valuable archive of this important interval of radical change on Planet Earth.

Geobiology of the Belcher Group: The Microfossil and Stromatolite Record

A remarkable fossil record of single-celled microbiota is preserved in peritidal stromatolitic dolostone of the Kasegalik and McLeary formations and granular iron formations of the Kipalu Formation (Moore 1918; LaBerge 1967; Hofmann and Jackson 1969, 1987; Hofmann 1974; Golubic and Hofmann 1976). Microbiota morphologies found in the Belcher Group include coccoid (i.e. spherical) and filamentous (i.e. segmented) chains of cells. Hofmann (1976) interpreted these as communities of benthic microbial organisms living in supratidal to subtidal environments. Although a microscope is required to view details of the microbiota, they can easily be seen on outcrops as stromatolites and microbialites, which are ubiquitous in most Belcher Group carbonate units. Stromatolites occur in the Kasegalik, McLeary, Tukarak, Mavor, Costello, and Rowatt formations. Microbialites (including stromatolites) form as a result of a benthic microbial community trapping and binding detrital sediment or precipitating as *in situ* minerals in shallow marine environments (e.g. Burne and Moore 1987). They are records of life rather than preserved examples of living organisms.

Broadly, stromatolite morphology is partly controlled by environmental factors, and thus it can indicate the depositional environment (e.g. Ricketts 1979) in conjunction with facies analysis. Hofmann (1976) identified distinct stromatolite morphologies representing four different taxa in the Belcher Group (*Minjaria*, *Lenia*, *Osagia* and *Vesicularites* groups). *Minjaria* only occurs in the Kasegalik Formation and is described as flat and digitate mats to large domes with some furcate and digitate branching (Fig. 22). All other morphologies are described in Hofmann (1977).

The McLeary Formation contains the highest diversity of stromatolite morphologies of any unit in the Belcher Group with a total of 13 taxa identified (Hofmann 1977; Ricketts 1979). Gabriel et al. (2021) discussed two of these stromatolite morphotypes from the McLeary Formation, as well as some of the mineralogical and geochemical details of the host rocks. The morphotypes include decimetre-size non-branching columnar to domal cherty stromatolites, and tabular bioherms of centimetre-size multifurcate, turbinata and anastomosed stromatolites. Some examples of stromatolite morphologies from the McLeary Formation are shown in Figure 22. These stromatolites have convex-upward laminae composed of alternating light and dark layers representing chert and micritic carbonate with variable amounts of organic carbon. As previously shown by Hofmann (1976), some chert formed early, demonstrated by kerogen laminations that overprint isopachous quartz, whereas further silica cementation occurred later with the formation of botryoidal quartz (Gabriel et al. 2021). Stromatolites in silty dolostone facies contain millimetre-scale dolomite granules, whereas decimetre-size domal to turbinata stromatolites contain pyrite as layers and centimetre-size pyrite concretions, stylolites and wavy microbial mat layers (Gabriel et al. 2021). Pyrite crystals likely formed during early diagenesis.

Preserved microfossils in the Belcher Group are found primarily in chert-replaced stromatolitic layers in dolostone, and this is attributed to silica cementation during early diagenesis (Hofmann 1976). The mat-forming *Eoentophysalis belcherensis* from the Kasegalik Formation is the oldest fossil cyanobacteria in the geological record (Hofmann 1976) at ca. 2015 Ma (Hodgkiss et al. 2019b). Hofmann (1976) interpreted the paleoenvironment in which the McLeary Formation was deposited to be intertidal mudflats and adjacent subtidal and supratidal

environments. Hofmann (1976) identified 10 different taxa from well-preserved microfossils and described various states of microfossil degradation.

Modern work on the Belcher microbiota has been sparse (Schopf et al. 2005; Dodd et al. 2018; Morrow-Pollock 2021) but is important. Such research used scanning electron microscopy, X-ray photoelectron microscopy and Raman spectroscopy to demonstrate biogenicity and to detect organic carbon in the rocks hosting the microbiota. Several of these studies now demonstrate the presence of organic carbon within structures that contain microfossils, including stromatolite laminae or spherules within the Kipalu Formation.

Microfossil Record of the Kasegalik and McLeary Formations

The microbiota of these carbonate-dominated formations is dominated by entophysalidaceans (*Eoentophysalis*) and other cyanobacterial genera (Hofmann 1976; Golubic and Hofmann 1976), which are morphologically simple, and resemble modern cyanobacteria living in shallow water settings (e.g. Suosaari et al. 2022). *Eoentophysalis belcherensis* is colony-forming and consists of spheroidal and ellipsoidal morphologies that occur in pairs, tetrads, and octets (Hofmann 1976), and is a probable precursor to modern *Entophysalis* sp. that still thrive in Hamelin Pool at Shark Bay, Australia (Suosaari et al. 2022).

Hofmann (1976) described microfossils from black chert layers, lenses, and nodules in peritidal stromatolitic dolostone of the Kasegalik and McLeary formations. Microbiota morphologies are generally spheroidal, ellipsoidal or filamentous. The spheroidal to ellipsoidal morphotypes are attributed to the genera *Eosynechococcus*, *Melasmatosphaera* and *Eoentophysalis* (Hofmann 1976). The cells of *Eosynechococcus* are either rod-like or ellipsoidal and range from 3 to 19 μm long to 1.2 to 7.5 μm wide (Hofmann 1976). Dark features (0.2 to 2 μm wide) occur within some cells and are interpreted as products of degradation of the cyanobacteria (Hofmann 1976). The cells of *Melasmatosphaera* are mainly solitary and a few microns to several tens of microns in diameters (Hofmann 1976). Dark inclusions (micron to sub-micron wide) within the cells are interpreted as products of degradation of the cyanobacteria (Hofmann 1976). The cells of *Eoentophysalis* are either spheroidal to elliptical or a sub-polyhedral shape and are 2.5 to 9 μm in diameter (Hofmann 1976). These cells occur as either solitary bunch clusters or as planar layers. Filamentous morphotypes are not as abundant as the spherical to ellipsoidal morphotypes, which is probably a function of the challenge of preserving their delicate structures through rock forming processes. Both *Rhiconema antiquum* and *Halythrix* sp. were identified and attributed to cyanobacteria by Hofmann (1976). Examples of the mat-forming cyanobacteria *Eoentophysalis belcherensis* and filamentous microfossils of probable cyanobacteria *Halythrix* sp. from Hofmann's (1976) specimens collected from the Kasegalik Formation are shown in Figure 20.

Gabriel et al. (2021) described filamentous structures in McLeary Formation stromatolites, and attributed these to the *Halythrix* sp., which Hofmann (1976) previously described from the Kasegalik Formation. The filamentous structures they described are either segmented and slightly coiled, occur within diagenetic chert (quartz) and are 25–70 μm long, and 4–6 μm wide, or they are about 200 μm long and associated with kerogen (organic carbon) in stromatolite laminae. Morrow-Pollock (2021) identified *Eoentophysalis belcherensis* microfossils in a new sample collected from the middle McLeary Formation.

Microfossil Record of the Kipalu Formation

Granular iron formations are typically interpreted to form as iron-rich sediments in high-energy, wave-agitated, shallow marine environments. However diagenetic or microbial processes could also have contributed to the formation of some types of granules. This is important to determine because the spherical nature of granules could indicate either physical or biological origin. An example of a contemporaneous granular iron formation unit that contains microbiota is the Gunflint Iron Formation in the Lake Superior region, U.S.A. (ca. 1.88 Ga). The Gunflint microbiota represents an assemblage of prokaryotic organisms preserved in black chert associated with stromatolites (Awramik and Barghoorn 1977).

In the earliest work, Moore (1918) described two morphologies present in the Kipalu iron formation, including a spherical form (0.5 to 10 μm in diameter), and a filamentous form composed of chains of spheroidal cells 1 to 2 μm across, both of which he compared to cyanobacteria. LaBerge (1967) documented ellipsoidal and spheroidal morphologies (5 to 40 μm in diameter) and their mineralogy within chert beds of the Kipalu iron formation.

Overall, the granules are composed predominantly of chert and hematite; the granule shapes are spheroidal to sub-rounded, or irregular sub-spheroidal shapes. Sand-sized quartz grains can occur within the chert between granules. Granules are dominantly composed of microcrystalline chert with grey or red hematite and minor siderite. Hematite can also occur as filaments between, within or emanating from granules (Dodd et al. 2018; Morrow-Pollock 2021). These hematite filaments are interpreted as microfossils that formed prior to diagenesis (Dodd et al. 2018), which infilled pore space with a silica cement (chert). Some granules contain organic matter, which occurs as micron-sized particles. Carbonate minerals including ankerite and dolomite can occur between the granules within the chert matrix (Dodd et al. 2018; Morrow-Pollock 2021).

The carbon isotopic compositions measured by Dodd et al. (2018) are typical of autotrophic CO_2 fixation and fractionation by the RuBisCo enzyme (Schidlowski 2001), and match typical values found in Paleoproterozoic organic matter. The carbon isotopic compositions are also similar to those produced by some iron-oxidizing bacteria (Kennedy et al. 2010). The organic matter in the Kipalu granular iron formation (Dodd et al. 2018; Morrow-Pollock 2021) and other contemporaneous rocks (e.g. Biwabik Formation, Minnesota) is interpreted to represent syngenetic organic matter, suggesting that microbes or their decayed remains might contribute to formation of the granules during diagenesis. Iron oxide, for example, can replace organic matter and microfossil cell walls during diagenesis (Shapiro and Konhauser 2015). Evidence from Raman spectroscopy that shows a strong dual peak signature and relative immaturity of the organic matter supports the syngenetic interpretation (Morrow-Pollock 2021).

A mechanical origin for the Kipalu Formation granules is supported by the presence of detrital minerals (e.g. quartz grains) and by cross-bedding in fine-grained sandstone within the unit. Dodd et al. (2018) suggested that mechanical reworking is important in forming the Kipalu granules, which might in part consist of silica colloids that formed haematitic–siliceous gels. They suggested the nucleus of the granules could have originated from iron-oxidizing bacteria. The presence of organic carbon, light carbon isotope values, and the presence of hematite filaments that were interpreted as microfossils by Dodd et al. (2018), all suggest a biological influence (Dodd et al. 2018; Morrow-Pollock 2021). Future work on the origin of these granules and microfossils present in the Belcher Group has the potential to advance our understanding of Paleoproterozoic geobiology. Additionally, further delineation of coeval seawater composition can help us understand the vital link between the role of atmospheric–oceanic oxygenation, trace metal composition and the evolution of metazoans (e.g. Butterfield 2015; Cole et al. 2020; Lyons et al. 2021), for which the Belcher Group provides many exciting research opportunities.

SUMMARY AND DISCUSSION

This paper outlines the geology of the Belcher Islands and highlights many of the features that make this region a site of great geological interest, especially with respect to this critical time interval in Earth history. Its geological heritage should be celebrated alongside its cultural, biological, and ecological significance in the pursuit of the Qikiqtait Protected Area project. Many of these features are visually striking, such as the stromatolites that occur in many of the carbonate rocks. Others are not so easily seen because fossils within the Belcher Group are microscopic. The geological features of the islands are an important part of their wider heritage and create spectacular landscapes. Although understanding of geological processes is not essential to enjoy such scenery, it does lend greater appreciation for its origins and significance.

Recent research is focused on amassing geochemical and geochronological information to put important biological, geochemical, and tectonic events into context. Nonetheless, understanding of ancient marine environments is of particular interest for future research. The McLeary and Mavor formations represent ancient carbonate reefs and tidal flats and contain many spectacular examples of primary depositional features that are well preserved. Given that the Belcher Group deposition coincided with a period of intense change in the state of the Earth's atmosphere, studying depositional environments where microbial activity is prominent, like a tidal flat environment (e.g. McLeary Formation) may provide much insight into these processes. As research into other planetary bodies continues, understanding the chemical conditions of the atmosphere and oceans during the early stages of Earth history will become increasingly important. The McLeary and Mavor formations in particular offer a unique opportunity to study those conditions and understand the primitive life-forms that ultimately transformed our own planet.

The Belcher Group also contains volcanic rocks that are of considerable interest to researchers. The Flaherty Formation represents a period of prolonged seafloor volcanism. The exceptional outcrop exposure, along with the large volumes of rock exposed, make the formation a world class locality for the study of ancient submarine volcanoes and volcanic systems.

The disappearance of banded iron formation and reappearance of granular iron formations after the Great Oxidation Event is an indication that atmospheric–oceanic oxygen levels and oceanic chemistry fluctuated throughout Earth's early history. The occurrence of granular iron formations during the Paleoproterozoic is a key indicator that atmospheric–oceanic oxygen levels did not increase in one step, but rather through a series of pulses that ultimately led us to present-day conditions. Although the iron ore deposits of the Kipalu Formation have not attracted the same level of exploration attention as other iron-bearing sequences of similar age, they are exceptionally well preserved and might yield many insights about the formation of these vital resources, and also the roles that primitive life forms might have played in their generation.

The physical characteristics preserved in the Belcher Group rocks are intriguing as well as their invisible resources that are of great scientific importance. The occurrences of the oldest cyanobacterial microfossil (*Eontophysalis belcherensis*) in the Kasegalik Formation near Churchill Sound and the McLeary Formation on Flaherty Island are presently unique in the geological record. The stromatolite structures that were built by these cyanobacteria are visually spectacular, especially in the McLeary Formation. These rocks and other parts of the Belcher Group will allow communities and future researchers the opportunity to better understand the geoheritage contained in the Belcher Islands.

ACKNOWLEDGEMENTS

Field work and scientific research on the Belcher Islands was made possible by the collaboration and assistance of many Sanikiluarmit in the community of Sanikiluaq, including Lisi Mikiyuk, Peter Novalinga, Anita Rumbolt, Gary Rumbolt, Allen Rumbolt, Jack Iqaluk, Puasi Ippak, Johnny Narlik, and Joel Heath; field work and assistance by students from the University of Saskatchewan (Zach Morrow-Pollock, Katie Klymyshyn, Chelsea Pastula, Bryna MacRae), Polar Knowledge Canada's Northern Scientific Training Program, and research grant funding from the Natural Sciences and Engineering Research Council of Canada (to C.A. Partin). This report was commissioned for the Arctic Eider Society as a part of background work for the Qikiqtait protected area project funded by the Nature Challenge Fund from Environment and Climate Change Canada.

REFERENCES

- Andres, M.S., and Reid R.P., 2006, Growth morphologies of modern marine stromatolites: A case study from Highborne Cay, Bahamas: *Sedimentary Geology*, v. 185, p. 319–328, <https://doi.org/10.1016/j.sedgeo.2005.12.020>.
- Ansdell, K.M., 2005, Tectonic evolution of the Manitoba-Saskatchewan segment of the Paleoproterozoic Trans-Hudson Orogen, Canada: *Canadian Journal of Earth Sciences*, v. 42, p. 741–759, <https://doi.org/10.1139/e05-035>.
- Arndt, N.T., and Todt, W., 1994, Formation of 1.9-Ga-old Trans-Hudson continental crust: Pb isotopic data: *Chemical Geology*, v. 118, p. 9–26, [https://doi.org/10.1016/0009-2541\(94\)90167-8](https://doi.org/10.1016/0009-2541(94)90167-8).
- Arndt, N.T., Brüggmann, G.E., Lehnert, K., Chauvel, C., and Chappell, B.W., 1987, Geochemistry, petrogenesis and tectonic environment of Circum-Superior Belt basalts, Canada: Geological Society, London, Special Publications, v. 33, p. 133–145, <https://doi.org/10.1144/GSL.SP.1987.033.01.10>.
- Aspler, L.B., and Chiarenzelli, J.R., 1998, Two Neoproterozoic supercontinents? Evidence from the Paleoproterozoic: *Sedimentary Geology*, v. 120, p. 75–104, [https://doi.org/10.1016/S0037-0738\(98\)00028-1](https://doi.org/10.1016/S0037-0738(98)00028-1).
- Awramik, S.M., and Barghoorn, E.S., 1977, The Gunflint microbiota: *Precambrian Research*, v. 5, p. 121–142, [https://doi.org/10.1016/0301-9268\(77\)90025-0](https://doi.org/10.1016/0301-9268(77)90025-0).
- Baragar, W.R.A., 2007, Geology, Ottawa Islands, eastern Hudson Bay, Nunavut: Geological Survey of Canada, A" Series Map, 2113A, <https://doi.org/10.4095/224569>.
- Baragar, W.R.A., and Scoates, R.F.J., 1981, The Circum-Superior Belt: A Proterozoic Plate Margin?, *in* Kröner, A., *ed.*, *Developments in Precambrian Geology*, v. 4, p. 297–330, [https://doi.org/10.1016/S0166-2635\(08\)70017-3](https://doi.org/10.1016/S0166-2635(08)70017-3).
- Baragar, W.R.A., and Scoates, R.F.J., 1987, Volcanic geochemistry of the northern segments of the Circum-Superior Belt of the Canadian Shield: Geological Society, London, Special Publications, v. 33, p. 113–131, <https://doi.org/10.1144/GSL.SP.1987.033.01.09>.
- Beauregard, M.A., and Ell, J., 2015, Nunavut carving stone deposit evaluation program: 2015 fieldwork at Rankin Inlet, Cumberland Sound and Arctic Bay, Nunavut: Canada-Nunavut Geoscience Office, Summary of Activities 2015, p. 183–192, <https://m.cngo.ca/wp-content/uploads/Summary-of-Activities-2015-P17-Beauregard.pdf>.

- Bell, R.T., and Jackson, G.D., 1974, Aphebian halite and sulphate indications in the Belcher Group, Northwest Territories: *Canadian Journal of Earth Sciences*, v. 11, p. 722–728, <https://doi.org/10.1139/e74-072>.
- Berman, R.G., Davis, W.J., and Pehrsson, S., 2007, Collisional Snowbird tectonic zone resurrected: Growth of Laurentia during the 1.9 Ga accretionary phase of the Hudsonian orogeny: *Geology*, v. 35, p. 911–914, <https://doi.org/10.1130/G23771A.1>.
- Bradley, D.C., 2008, Passive margins through earth history: *Earth-Science Reviews*, v. 91, p. 1–26, <https://doi.org/10.1016/j.earscirev.2008.08.001>.
- Burne, R.V., and Moore, L.S., 1987, Microbialites: organosedimentary deposits of benthic microbial communities: *Palaios*, v. 2, p. 241–254, <https://doi.org/10.2307/3514674>.
- Butterfield, N.J., 2015, Proterozoic photosynthesis—a critical review: *Palaeontology*, v. 58, p. 953–972, <https://doi.org/10.1111/pala.12211>.
- Canfield, D.E., van Zuilen, M.A., Nabhan, S., Bjerrum, C.J., Zhang, S., Wang, H., and Wang, X., 2021, Petrographic carbon in ancient sediments constrains Proterozoic Era atmospheric oxygen levels: *Proceedings of the National Academy of Sciences*, v. 118, e2101544118, <https://doi.org/10.1073/pnas.2101544118>.
- Catling, D.C., and Zahnle, K.J., 2020, The Archean atmosphere: *Science Advances*, v. 6, eaax1420, <https://doi.org/10.1126/sciadv.aax1420>.
- Chandler, F.W., 1984, Metallogenesis of an early Proterozoic foreland sequence, eastern Hudson Bay, Canada: *Journal of the Geological Society*, v. 141, p. 299–313, <https://doi.org/10.1144/gsjgs.141.2.0299>.
- Chandler, F.W., 1988, The early Proterozoic Richmond Gulf graben, east coast of Hudson Bay, Quebec: *Geological Survey of Canada, Bulletin No. 362*, 76 p., <https://doi.org/10.4095/126313>.
- Chandler, F.W., and Parrish, R.R., 1989, Age of the Richmond Gulf Group and implications for rifting in the Trans-Hudson Orogen, Canada: *Precambrian Research*, v. 44, p. 277–288, [https://doi.org/10.1016/0301-9268\(89\)90048-X](https://doi.org/10.1016/0301-9268(89)90048-X).
- Chauvel, C., Arndt, N.T., Kielinzcuk, S., and Thom, A., 1987, Formation of Canadian 1.9 Ga old continental crust. I: Nd isotopic data: *Canadian Journal of Earth Sciences*, v. 24, p. 396–406, <https://doi.org/10.1139/e87-042>.
- Ciborowski, T.J.R., Minifie, M.J., Kerr, A.C., Ernst, R.E., Baragar, B., and Millar, I.L., 2017, A mantle plume origin for the Palaeoproterozoic Circum-Superior Large Igneous Province: *Precambrian Research*, v. 294, p. 189–213, <https://doi.org/10.1016/j.precamres.2017.03.001>.
- Cole, D.B., Mills, D.B., Erwin, D.H., Sperling, E.A., Porter, S.M., Reinhard, C.T., and Planavsky, N.J., 2020, On the co-evolution of surface oxygen levels and animals: *Geobiology*, v. 18, p. 260–281, <https://doi.org/10.1111/gbi.12382>.
- Corrigan, D., Pehrsson, S., Wodicka, N., and de Kemp, E., 2009, The Palaeoproterozoic Trans-Hudson Orogen: a prototype of modern accretionary processes: *Geological Society, London, Special Publications*, v. 327, p. 457–479, <https://doi.org/10.1144/SP327.19>.
- Corrigan, D., van Rooyen, D., and Wodicka, N., 2021, Indenter tectonics in the Canadian Shield: A case study for Paleoproterozoic lower crust exhumation, orocline development, and lateral extrusion: *Precambrian Research*, v. 355, 106083, <https://doi.org/10.1016/j.precamres.2020.106083>.
- Dimroth, E., Baragar, W.R.A., Bergeron, R., and Jackson, G.D., 1970, The filling of the Circum-Ungava geosyncline, *in* Baer, A.J., *ed.*, *Symposium on Basins and Geosynclines of the*

- Canadian Shield: Geological Survey of Canada, Paper 70-40, p. 45–142, <https://doi.org/10.4095/124922>.
- Dodd, M.S., Papineau, D., She, Z., Fogel, M.L., Nederbragt, S., and Pirajno, F., 2018, Organic remains in late Palaeoproterozoic granular iron formations and implications for the origin of granules: *Precambrian Research*, v. 310, p. 133–152, <https://doi.org/10.1016/j.precamres.2018.02.016>.
- Donaldson, J.A., and Ricketts, B.D., 1979, Beachrock in Proterozoic dolostone of the Belcher Islands, Northwest Territories, Canada: *Journal of Sedimentary Research*, v. 49, p. 1287–1294, <https://doi.org/10.1306/212F790F-2B24-11D7-8648000102C1865D>.
- Dyke, A.S., Andrews, J.T., Clark, P.U., England, J.H., Miller, G.H., Shaw, J., and Veillette, J.J., 2002, The Laurentide and Innuitian ice sheets during the Last Glacial Maximum: *Quaternary Science Reviews*, v. 21, p. 9–31, [https://doi.org/10.1016/S0277-3791\(01\)00095-6](https://doi.org/10.1016/S0277-3791(01)00095-6).
- Ernst, R.E., and Bell, K., 2010, Large igneous provinces (LIPs) and carbonatites: *Mineralogy and Petrology*, v. 98, p. 55–76, <https://doi.org/10.1007/s00710-009-0074-1>.
- Evans, D.A.D., and Mitchell, R.N., 2011, Assembly and breakup of the core of Paleoproterozoic–Mesoproterozoic supercontinent Nuna: *Geology*, v. 39, p. 443–446, <https://doi.org/10.1130/G31654.1>.
- Flaherty, R.J., 1918, The Belcher Islands of Hudson Bay: their discovery and exploration: *Geographical Review*, v. 5, p. 433–458, <https://doi.org/10.2307/207804>.
- Fralick, P., Davis, D.W., and Kissin, S.A., 2002, The age of the Gunflint Formation, Ontario, Canada: single zircon U–Pb age determinations from reworked volcanic ash: *Canadian Journal of Earth Sciences*, v. 39, p. 1085–1091, <https://doi.org/10.1139/e02-028>.
- Frisch, T., 2021, Garth Digby Jackson (1929–2021): *Arctic*, v. 74, p. 564–565, <https://doi.org/10.14430/arctic74148>.
- Fryer, B.J., 1972, Age determinations in the Circum–Ungava Geosyncline and the evolution of Precambrian Banded Iron-Formations: *Canadian Journal of Earth Sciences*, v. 9, p. 652–663, <https://doi.org/10.1139/e72-055>.
- Gabriel, N.W., Papineau, D., She, Z., Leider, A., and Fogel, M.L., 2021, Organic diagenesis in stromatolitic dolomite and chert from the late Palaeoproterozoic McLeary Formation: *Precambrian Research*, v. 354, 106052, <https://doi.org/10.1016/j.precamres.2020.106052>.
- Gauthier, M.S., Hodder, T.J., Ross, M., Kelley, S.E., Rochester, A., and McCausland, P., 2019, The subglacial mosaic of the Laurentide Ice Sheet; a study of the interior region of southwestern Hudson Bay: *Quaternary Science Reviews*, v. 214, p. 1–27, <https://doi.org/10.1016/j.quascirev.2019.04.015>.
- Golubic, S., and Hofmann, H.J., 1976, Comparison of Holocene and mid-Precambrian Entophysalidaceae (Cyanophyta) in stromatolitic algal mats: cell division and degradation: *Journal of Paleontology*, v. 50, p. 1074–1082, <https://www.jstor.org/stable/1303548>.
- Gross, G.A., 2009, Iron formation in Canada, genesis and geochemistry: Geological Survey of Canada, Open File No. 5987, 164 p., <https://doi.org/10.4095/226638>.
- Hamilton, M.A., Buchan, K.L., Ernst, R.E., and Scott, G.M., 2009, Widespread and short-lived 1870 Ma mafic magmatism along the northern Superior Craton margin (Abstract), American Geophysical Union-Geological Association of Canada, Joint Assembly, 24–27 May 2009, Toronto, ON, Abstract GA11A-01.
- Haycock-Chavez, N., 2021, Indigenous-driven conservation: exploring the planning of Qikiqtait protected area in Sanikiluaq, Nunavut: MSc thesis, Memorial University, St. John's NL, 124 p., <https://doi.org/10.48336/KTC1-AV62>.

- Hodgskiss, M.S.W., and Sperling, E.A., 2020, Stratigraphy and shale geochemistry of the Belcher Group, Belcher Islands, southern Nunavut: Canada-Nunavut Geoscience Office, Summary of Activities 2019, p. 65–78, <https://cngo.ca/summary-of-activities/2019/>.
- Hodgskiss, M.S.W., and Sperling, E.A., 2022, A prolonged, two-step oxygenation of Earth's early atmosphere: Support from confidence intervals: *Geology*, v. 50, p. 158–162, <https://doi.org/10.1130/G49385.1>.
- Hodgskiss, M.S.W., Crockford, P.W., Peng, Y., Wing, B.A., and Horner, T.J., 2019a, A productivity collapse to end Earth's Great Oxidation: *Proceedings of the National Academy of Sciences*, v. 116, p. 17207–17212, <https://doi.org/10.1073/pnas.1900325116>.
- Hodgskiss, M.S.W., Dagnaud, O.M.J., Frost, J.L., Halverson, G.P., Schmitz, M.D., Swanson-Hysell, N.L., and Sperling, E.A., 2019b, New insights on the Orosirian carbon cycle, early Cyanobacteria, and the assembly of Laurentia from the Paleoproterozoic Belcher Group: *Earth and Planetary Science Letters*, v. 520, p. 141–152, <https://doi.org/10.1016/j.epsl.2019.05.023>.
- Hodgskiss, M.S.W., Lalonde, S.V., Crockford, P.W., and Hutchings, A.M., 2021, A carbonate molybdenum isotope and cerium anomaly record across the end-GOE: Local records of global oxygenation: *Geochimica et Cosmochimica Acta*, v. 313, p. 313–339, <https://doi.org/10.1016/j.gca.2021.08.013>.
- Hoffman, P.F., 1985, Is the Cape Smith belt (northern Quebec) a klippe?: *Canadian Journal of Earth Sciences*, v. 22, p. 1361–1369, <https://doi.org/10.1139/e85-140>.
- Hoffman, P.F., 1987, Early Proterozoic foredeeps, foredeep magmatism, and Superior-type iron-formations of the Canadian Shield, *in* Kröner, A., *ed.*, *Proterozoic Lithospheric Evolution: Geodynamics Series*, v. 17, p. 85–98, <https://doi.org/10.1029/GD017p0085>.
- Hoffman, P.F., 1988, United Plates of America, the birth of a craton: Early Proterozoic assembly and growth of Laurentia: *Annual Review of Earth and Planetary Sciences*, v. 16, p. 543–603, <https://doi.org/10.1146/annurev.earth.16.050188.002551>.
- Hoffman, P.F., 1990, Dynamics of the tectonic assembly of northeast Laurentia in geon 18 (1.9–1.8 Ga): *Geoscience Canada*, v. 17, p. 222–226, <https://journals.lib.unb.ca/index.php/GC/article/view/3692>.
- Hofmann, H.J., 1971, Precambrian fossils, pseudofossils and problematica in Canada: *Geological Survey of Canada, Bulletin No. 189*, 146 p., <https://doi.org/10.4095/123948>.
- Hofmann, H.J., 1974, Mid-Precambrian prokaryotes(?) from the Belcher Islands, Canada: *Nature*, v. 249, p. 87–88, <https://doi.org/10.1038/249087a0>.
- Hofmann, H.J., 1976, Precambrian microflora, Belcher Islands, Canada: Significance and systematics: *Journal of Paleontology*, v. 50, p. 1040–1073, <https://www.jstor.org/stable/1303547>.
- Hofmann, H.J., 1977, On Aphebian stromatolites and Riphean stromatolite stratigraphy: *Precambrian Research*, v. 5, p. 175–205, [https://doi.org/10.1016/0301-9268\(77\)90027-4](https://doi.org/10.1016/0301-9268(77)90027-4).
- Hofmann, H.J., and Jackson, G.D., 1969, Precambrian (Aphebian) microfossils from Belcher Islands, Hudson Bay: *Canadian Journal of Earth Sciences*, v. 6, p. 1137–1144, <https://doi.org/10.1139/e69-115>.
- Hofmann, H.J., and Jackson, G.D., 1987, Proterozoic ministromatolites with radial-fibrous fabric: *Sedimentology*, v. 34, p. 963–971, <https://doi.org/10.1111/j.1365-3091.1987.tb00586.x>.
- House of Commons Standing Committee on Fisheries and Oceans, 2023, Report 9: Main Estimates 2023–24: Votes 1, 5 and 10 under Department of Fisheries and Oceans: House of

- Commons, Canada, Meeting March 27, 2023, <https://www.ourcommons.ca/Committees/en/FOPO/StudyActivity?studyActivityId=12073274>.
- Hynes, A., 1991, The gravity field of eastern Hudson Bay: Evidence for a flexural origin for the Hudson Bay (Nastapoka) Arc?: *Tectonics*, v. 10, p. 722–728, <https://doi.org/10.1029/91TC00643>.
- Jackson, G.D., 1960, Belcher Islands, Northwest Territories, 33M, 34D, and E: Geological Survey of Canada, Paper 60-20, 13 p., <https://doi.org/10.4095/101205>.
- Jackson, G.D., 2013, Geology, Belcher Islands, Nunavut: Geological Survey of Canada, Open File 4923, 159 p., <https://doi.org/10.4095/292434>.
- Karhu, J.A., and Holland, H.D., 1996, Carbon isotopes and the rise of atmospheric oxygen: *Geology*, v. 24, p. 867–870, [https://doi.org/10.1130/0091-7613\(1996\)024%3C0867:CIATRO%3E2.3.CO;2](https://doi.org/10.1130/0091-7613(1996)024%3C0867:CIATRO%3E2.3.CO;2).
- Kennedy, C.B., Gault, A.G., Fortin, D., Clark, I.D., Pedersen, K., Scott, S.D., and Ferris, F.G., 2010, Carbon isotope fractionation by circumneutral iron-oxidizing bacteria: *Geology*, v. 38, p. 1087–1090, <https://doi.org/10.1130/G30986.1>.
- Konhäuser, K.O., Planavsky, N.J., Hardisty, D.S., Robbins, L.J., Warchola, T.J., Haugaard, R., Lalonde, S.V., Partin, C.A., Oonk, P.B.H., Tsikos, H., Lyons, T.W., Bekker, A., and Johnson, C.M., 2017, Iron formations: A global record of Neoproterozoic to Palaeoproterozoic environmental history: *Earth-Science Reviews*, v. 172, p. 140–177, <https://doi.org/10.1016/j.earscirev.2017.06.012>.
- Laarman, J.E., 2004, Soapstone occurrences on Tukarak Island: A product of plume tectonics on the east margin of the Trans Hudson Orogen, Belcher Islands, Nunavut: Unpublished BSc thesis, Western University, ON.
- LaBerge, G.L., 1967, Microfossils and Precambrian iron-formations: *Geological Society of America Bulletin*, v. 78, p. 331–342, [https://doi.org/10.1130/0016-7606\(1967\)78\[331:MAPI\]2.0.CO;2](https://doi.org/10.1130/0016-7606(1967)78[331:MAPI]2.0.CO;2).
- Laznicka, P., 2014, Giant metallic deposits—A century of progress: *Ore Geology Reviews*, v. 62, p. 259–314, <https://doi.org/10.1016/j.oregeorev.2014.03.002>.
- Legault, F., 1993, The petrogenesis of Proterozoic continental volcanism in the Belcher Islands with implications for the evolution of the Circum-Ungava Fold Belt: Unpublished MSc thesis, McGill University, QC, 112 p.
- Legault, F., Francis, D., Hynes, A., and Budkewitsch, P., 1994, Proterozoic continental volcanism in the Belcher Islands: implications for the evolution of the Circum Ungava Fold Belt: *Canadian Journal of Earth Sciences*, v. 31, p. 1536–1549, <https://doi.org/10.1139/e94-136>.
- Leggett, S.R., 1974, A petrographic and stratigraphic study of the Flaherty Formation, Belcher Islands, Northwest Territories: Unpublished BSc thesis, Brock University, ON.
- Lyons, T.W., Diamond, C.W., Planavsky, N.J., Reinhard, C.T., and Li, C., 2021, Oxygenation, life, and the planetary system during Earth's middle history: An overview: *Astrobiology*, v. 21, p. 906–923, <https://doi.org/10.1089/ast.2020.2418>.
- McDonald, B.S., Partin, C.A., Nadeau, M.D., and Higgins, J.A., 2022, Unraveling Paleoproterozoic seawater chemistry from early diagenetic dolomite of the Belcher Group, Nunavut, Canada using $\delta^{26}\text{Mg}$ (Abstract): *Geoscience Canada*, v. 49, p. 159–160, <https://doi.org/10.12789/geocanj.2022.49.188>.

- Moore, E.S., 1918, The iron-formation on Belcher Islands, Hudson Bay, with special reference to its origin and its associated algal limestones: *The Journal of Geology*, v. 26, p. 412–438, <https://doi.org/10.1086/622604>.
- Morrow-Pollock, Z.S.W., 2021, The geobiology of the Paleoproterozoic Belcher Group, Nunavut, Canada: MSc Thesis, University of Saskatchewan, SK, 361 p., <https://hdl.handle.net/10388/13389>.
- Mukhopadhyay, M., and Gibb, R.A., 1981, Gravity anomalies and deep structure of eastern Hudson Bay: *Tectonophysics*, v. 72, p. 43–60, [https://doi.org/10.1016/0040-1951\(81\)90086-X](https://doi.org/10.1016/0040-1951(81)90086-X).
- Nunavut Planning Commission, 2021, Leading the way through land use planning: Nunavut Planning Commission, Draft July 2021, 103 p., https://www.nunavut.ca/sites/default/files/21-001e-2021-07-08-2021_draft_nunavut_land_use_plan-english.pdf.
- Partin, C.A., 2023, A tectonic context for fluctuations in late Paleoproterozoic oxygen content, *in* Whitmeyer, S.J., Williams, M.L., Kellett, D.A., and Tikoff, B., *eds.*, *Laurentia: Turning Points in the Evolution of a Continent: Geological Society of America Memoir*, v. 220, p. 111–121, [https://doi.org/10.1130/2022.1220\(07\)](https://doi.org/10.1130/2022.1220(07)).
- Partin, C.A., Bekker, A., Planavsky, N.J., Scott, C.T., Gill, B.C., Li, C., Podkovyrov, V., Maslov, A., Konhauser, K.O., Lalonde, S.V., Love, G.D., Poulton, S.W., and Lyons, T.W., 2013, Large-scale fluctuations in Precambrian atmospheric and oceanic oxygen levels from the record of U in shales: *Earth and Planetary Science Letters*, v. 369–370, p. 284–293, <https://doi.org/10.1016/j.epsl.2013.03.031>.
- Pastula, C., and Partin, C.A., 2023, What are omars? (Poster): Saskatchewan Geological Open House, November 27–29, 2023, Saskatoon, SK.
- Percival, J.A., 2007, Geology and metallogeny of the Superior Province, Canada, *in* Goodfellow, W.D., *ed.*, *Mineral Deposits of Canada: A Synthesis of Major Deposit-Types, District Metallogeny, the Evolution of Geological Provinces, and Exploration Methods: Geological Association of Canada, Mineral Deposits Division, Special Publication no. 5*, p. 903–928.
- Poulton, S.W., Fralick, P.W., and Canfield, D.E., 2010, Spatial variability in oceanic redox structure 1.8 billion years ago: *Nature Geoscience*, v. 3, p. 486–490, <https://doi.org/10.1038/ngeo889>.
- Poulton, S.W., Bekker, A., Cumming, V.M., Zerkle, A.L., Canfield, D.E., and Johnston, D.T., 2021, A 200-million-year delay in permanent atmospheric oxygenation: *Nature*, v. 592, p. 232–236, <https://doi.org/10.1038/s41586-021-03393-7>.
- Prest, V.K., 1990, Laurentide ice-flow patterns: A historical review, and implications of the dispersal of Belcher Islands erratics: *Géographie physique et Quaternaire*, v. 44, p. 113–136, <https://doi.org/10.7202/032812ar>.
- Prest, V.K., Donaldson, J.A., and Mooers, H.D., 2000, The omar story: the role of omars in assessing glacial history of west-central North America: *Géographie physique et Quaternaire*, v. 54, p. 257–270, <https://doi.org/10.7202/005654ar>.
- Regis, D., Pehrsson, S., Martel, E., Thiessen, E., Peterson, T., and Kellett, D., 2021, Post-1.9 Ga evolution of the south Rae craton (Northwest Territories, Canada): A Paleoproterozoic orogenic collapse system: *Precambrian Research*, v. 355, 106105, <https://doi.org/10.1016/j.precamres.2021.106105>.
- Ricketts, B.D., 1979, Sedimentology and stratigraphy of eastern and central Belcher Islands, Northwest Territories: PhD thesis, Carleton University, ON, 314 p., <https://doi.org/10.22215/etd/1979-00451>.

- Ricketts, B.D., 1981, A submarine fan–distal molasse sequence of Middle Precambrian age, Belcher Islands, Hudson Bay: *Bulletin of Canadian Petroleum Geology*, v. 29, p. 561–582, <https://doi.org/10.35767/gscpgbull.29.4.561>.
- Ricketts, B.D., 1983, The evolution of a middle Precambrian dolostone sequence; a spectrum of dolomitization regimes: *Journal of Sedimentary Research*, v. 53, p. 565–586, <https://doi.org/10.1306/212F8238-2B24-11D7-8648000102C1865D>.
- Ricketts, B.D., and Donaldson, J.A., 1981, Sedimentary history of the Belcher Group of Hudson Bay, *in* Campbell, F.H.A., *ed.*, Proterozoic Basins of Canada: Geological Survey of Canada, Paper 81-10, p. 235–254, <https://doi.org/10.4095/109385>.
- Ricketts, B.D., and Donaldson, J.A., 1989, Stromatolite reef development on a mud-dominated platform in the Middle Precambrian Belcher Group of Hudson Bay, *in* Geldsetzer, H.H.J., James, N.P., and Tebbutt, G.E., *eds.*, Reefs, Canada and Adjacent area: Canadian Society of Petroleum Geologists Memoir, v. 13, p. 113–119.
- Ricketts, B.D., Ware, M.J., and Donaldson, J.A., 1982, Volcaniclastic rocks and volcaniclastic facies in the Middle Precambrian (Aphebian) Belcher Group, Northwest Territories, Canada: *Canadian Journal of Earth Sciences*, v. 19, p. 1275–1294, <https://doi.org/10.1139/e82-109>.
- Roksandic, M.M., 1987, The tectonics and evolution of the Hudson Bay region, *in* Beaumont, C., and Tankard, A.J., *eds.*, Sedimentary Basins and Basin-Forming Mechanisms: Canadian Society of Petroleum Geologists Memoir, v. 12, p. 507–518.
- Sanikiluaq Qikiqtait Steering Committee, 2021, Implementing Sanikiluaq’s vision for a Qikiqtait guardians’ program: program overview: Sanikiluaq, NU.
- Schidlowski, M., 2001, Carbon isotopes as biogeochemical recorders of life over 3.8 Ga of Earth history: evolution of a concept: *Precambrian Research*, v. 106, p. 117–134, [https://doi.org/10.1016/S0301-9268\(00\)00128-5](https://doi.org/10.1016/S0301-9268(00)00128-5).
- Schneider, D.A., Bickford, M.E., Cannon, W.F., Schulz, K.J., and Hamilton, M.A., 2002, Age of volcanic rocks and syndepositional iron formations, Marquette Range Supergroup: implications for the tectonic setting of Paleoproterozoic iron formations of the Lake Superior region: *Canadian Journal of Earth Sciences*, v. 39, p. 999–1012, <https://doi.org/10.1139/e02-016>.
- Schopf, J.W., Kudryavtsev, A.B., Agresti, D.G., Czaja, A.D., and Wdowiak, T.J., 2005, Raman imagery: a new approach to assess the geochemical maturity and biogenicity of permineralized Precambrian fossils: *Astrobiology*, v. 5, p. 333–371, <https://doi.org/10.1089/ast.2005.5.333>.
- Shapiro, R.S., and Konhauser, K.O., 2015, Hematite-coated microfossils: primary ecological fingerprint or taphonomic oddity of the Paleoproterozoic?: *Geobiology*, v. 13, p. 209–224, <https://doi.org/10.1111/gbi.12127>.
- Sherman, A.G., 1993, Anatomy of giant stromatolite mounds in the Paleoproterozoic Mavor Formation, Belcher Islands, Northwest Territories: Unpublished MSc thesis, Université de Montréal, QC.
- Skipton, D.R., St-Onge, M.R., Kellett, D.A., Joyce, N.L., and Smith, S., 2023, Rapid postorogenic cooling of the Paleoproterozoic Cape Smith foreland thrust belt and footwall Archean basement, Trans-Hudson orogen, Canada, *in* Whitmeyer, S.J., Williams, M.L., Kellett, D.A., and Tikoff, B., *eds.*, Laurentia: Turning Points in the Evolution of a Continent: Geological Society of America Memoirs, v. 220, [https://doi.org/10.1130/2022.1220\(06\)](https://doi.org/10.1130/2022.1220(06)).

- Steenkamp, H.M., Timlick, L., Elgin, R.A., and Akavak, M., 2016, Geological mapping and petrogenesis of carving stone in the Belcher Islands, Nunavut: Canada-Nunavut Geoscience Office, Summary of Activities 2016, p. 121–130.
- Steenkamp, H.M., Elgin, R.A., and Therriault, I., 2017, Geological mapping and resource evaluation of the Koonark carving stone deposit, northern Baffin Island, Nunavut: Canada-Nunavut Geoscience Office, Summary of Activities 2017, p. 139–149.
- St-Onge, M.R., and Ijewliw, O.J., 1996, Mineral corona formation during high-P retrogression of granulitic rocks, Ungava Orogen, Canada: *Journal of Petrology*, v. 37, p. 553–582, <https://doi.org/10.1093/petrology/37.3.553>.
- St-Onge, M.R., and Lucas, S.B., 1991, Evolution of regional metamorphism in the Cape Smith Thrust Belt (northern Quebec, Canada): interaction of tectonic and thermal processes: *Journal of Metamorphic Geology*, v. 9, p. 515–534, <https://doi.org/10.1111/j.1525-1314.1991.tb00545.x>.
- St-Onge, M.R., Scott, D.J., and Lucas, S.B., 2000, Early partitioning of Quebec: Microcontinent formation in the Paleoproterozoic: *Geology*, v. 28, p. 323–326, [https://doi.org/10.1130/0091-7613\(2000\)28%3C323:EPOQMF%3E2.0.CO;2](https://doi.org/10.1130/0091-7613(2000)28%3C323:EPOQMF%3E2.0.CO;2).
- St-Onge, M.R., van Gool, J.A.M., Garde, A.A., and Scott, D.J., 2009, Correlation of Archaean and Palaeoproterozoic units between northeastern Canada and western Greenland: constraining the pre-collisional upper plate accretionary history of the Trans-Hudson orogen, in Cawood, R.A., and Kröner, A., eds., *Earth Accretionary Systems in Space and Time*: Geological Society, London, Special Publications, v. 318, p. 193–235, <https://doi.org/10.1144/SP318.7>.
- Suosaari, E.P., Reid, R.P., Mercadier, C., Vitek, B.E., Oehlert, A.M., Stolz, J.F., Giusfredi, P.E., and Eberli, G.P., 2022, The microbial carbonate factory of Hamelin Pool, Shark Bay, Western Australia: *Scientific Reports*, v. 12, 12902, <https://doi.org/10.1038/s41598-022-16651-z>.
- Timlick, L., Steenkamp, H.M., and Camacho, A.L., 2017, Comparative study of the petrogenesis of excellent-quality carving stone from Korok Inlet, southern Baffin Island and the Belcher Islands, Nunavut: Canada-Nunavut Geoscience Office, Summary of Activities 2017, p. 129–138.
- Todt, W.A., Chauvel, C., Arndt, N.T., and Hoffman, A.W., 1984, Pb isotopic composition and age of Proterozoic komatiites and related rocks from Canada (Abstract): EOS, 1984 Fall Meeting, v. 65, p. 1129.
- Wahl, G.J., 2012, Haig Inlet iron project technical report, Belcher Islands, Qikiqtaaluk Region, Nunavut, Canada: GH Wahl & Associates Consulting for Canadian Orebodies Incorporated, 62 p.
- Wanless, R.K., Stevens, R.D., Lachance, G.R., and Rimsaite, R.Y.H., 1965, Age determinations and geological studies, Part 1-Isotopic Ages, Report 5: Geological Survey of Canada, Paper 64-17, 126 p., <https://doi.org/10.4095/101021>.
- Wanless, R.K., Stevens, R.D., Lachance, G.R., and Edmonds, C.M., 1967, Age determinations and geological studies, K-Ar isotope ages, Report 7: Geological Survey of Canada, Paper 66-17, 120 p., <https://doi.org/10.4095/100968>.
- Wanless, R.K., Stevens, R.D., Lachance, G.R., and Edmonds, C.M., 1968, Age determinations and geological studies, K-Ar isotope ages, Report 8: Geological Survey of Canada, Paper 67-2A, 141 p., <https://doi.org/10.4095/103342>.

- Weller, O.M., and St-Onge, M.R., 2017, Record of modern-style plate tectonics in the Palaeoproterozoic Trans-Hudson orogen: *Nature Geoscience*, v. 10, p. 305–311, <https://doi.org/10.1038/NGEO2904>.
- Young, G.A., 1922, Iron-bearing rocks of Belcher Islands, Hudson Bay: Geological Survey of Canada, Summary Report, 1921, Part E, 61 p., <https://doi.org/10.4095/103426>.

Received April 2023

Accepted as revised January 2024

FIGURE CAPTIONS

Figure 1. Simplified geological map of North America and Greenland showing the orientation of Archean and Paleoproterozoic cratons. Abbreviations: CS, Cape Smith belt; K, Ketilidian; N, Nagssugtoqidian orogen; NAC, North Atlantic craton; NQ, New Quebec orogen; MI, Meta Incognita microcontinent; SECP, Southeastern Churchill Province; SL, Slave craton; T, Torngat orogen; U, Ungava indenter; WY, Wyoming craton. Red star denotes the location of the Belcher Islands in Hudson Bay. Modified from Corrigan et al. (2021).

Figure 2. A, geological map of the Belcher Islands; B, map of central Canada and Hudson Bay region with the location of the Belcher Islands indicated (modified from Prest et al. 2000); C, corresponding cross-section along the A–B line. Modified from Jackson (2013).

Figure 3. Simplified stratigraphic column of the Belcher Group. Modified after Ricketts (1979).
1 Youngest detrital zircon U–Pb age (Corrigan et al. 2021)
2 U–Pb zircon crystallization age from tuffaceous shale (Hodgskiss et al. 2019a)
3 U–Pb baddeleyite crystallization age from Haig intrusion (Hamilton et al. 2009)

Figure 4. Compilation of dominant Kasegalik Formation sedimentary structures and rock types. A, red argillite facies; B, thinly laminated, light grey dolomicrite; C, silty dolomicrite laths stacked-edge wise and suspended within a dolomicrite matrix; D, sulphate molds; E, thinly laminated dolomicrite preserving a broad stromatolitic mound; F, branching to non-branching columnar stromatolites within a grey–pink matrix of dolomicrite.

Figure 5. Compilation of Eskimo Formation rock types and volcanic textures. A, laminated green to pale green mafic tuff; B, parallel to cross-bedded mafic tuff; C, massive basalt containing plagioclase phenocrysts of varying size; D, volcanic breccia; E, plagioclase-phyric flow as described in Legault et al. (1994).

Figure 6. Compilation of Fairweather Formation sedimentary structures and rock types. A, B, thinly laminated dolostone unit found at the base of the Fairweather Formation.; C, outcrop photo depicting alternating beds of silty dolomicrite and red argillite (thin beds); D, thinly laminated green argillite with intercalated white clay layers; E, unidirectional ripple structure; F, channel-fill conglomerate composed of silty dolomicrite clasts of varying size with a coarse-grained sandstone fill.

Figure 7. Compilation of McLeary Formation sedimentary structures and rock types. A, cross-stratified sandy dolomicrite facies found in the basal portion of the middle member; B, an

example of the many beds of reworked dolomicrite laths and pisoliths; C, D, examples of mini-digitate stromatolites taken to at the contact between the middle and upper members; E–I, stromatolite morphologies found within the middle and upper members of the formation; F, non-branching columnar and domal stromatolites; G, an example of the characteristic conical shape of a *Conophyton*; H, chert-replaced stromatolite; I, distinctly buff-orange, stromatolite-rich marker bed that denotes the top of the McLeary Formation.

Figure 8. Compilation of Tukarak Formation sedimentary structures and rock types. A, B, examples of the characteristic maroon-coloured wavy planar bedding that makes the Tukarak Formation a unique marker bed; C, D, outcrop image of the contact between the upper Tukarak Formation and the overlying Mavor Formation, images are looking north and west, respectively and taken about 3 km south of the Hudson Bay Company camp on Tukarak Island (HBC Outpost located on Figure 2); E, lenses of silty dolomicrite within thinly laminated argillite; F, buff, silty dolomicrite laminations located near the contact with the overlying Mavor Formation; G, angular clasts of silty dolomicrite encapsulated by a matrix of silty dolomicrite, bounded by thickly laminated beds of red argillite.

Figure 9. Compilation of main Mavor Formation sedimentary structures and rock types. A, alternating beds of grey and buff weathered dolomicrite with parallel to ripple laminations (staff is 1.5 m); B, grainstone bed containing pisoids and rip-up clasts; C, grainstone bed with brecciated microbial laminations found near the base of the Mavor Formation; D, an example of flaser bedding; E, an example of a stylolite formed due to pressure dissolution in response to burial (white arrow); F, an example of domal stromatolites found throughout the Mavor Formation.; G, metre-scale domal stromatolite; H, bedding-parallel surface of stromatolitic mounds, depicting the 3-dimensional orientation of the bulbous mounds.

Figure 10. Drone photomosaic of the Costello Formation on southeastern Mavor Island (Fig. 10 located on Figure 2) illustrating both the poor exposure of the lower shale beds (immediately above the Mavor–Costello contact) as well as the stark colour contrast between the buff-coloured beds of the lower 100 m and the maroon-coloured beds of the upper beds.

Figure 11. Compilation of main Costello Formation sedimentary structures and rock types. A, an example of the grey to black shale beds found at the base of the Costello Formation.; B, example of the nodular calcite interbeds that are ultimately responsible for the corrugated texture observed in the Costello Formation; C, image of an intraformational conglomerate found near the top of the formation; D, slump fold near the contact with the overlying Laddie Formation.

Figure 12. An example of the characteristically red colour of the argillite facies found within the Laddie Formation.

Figure 13. Compilation of main Rowatt Formation sedimentary structures and lithologies. A, typical grainstone facies at the base of the upper member; B, trough cross-bedded sandstone found near the base of the formation; C, conglomerate facies preserving cross-stratification; D, clasts of dolomicrite surrounded by a silty dolomicrite matrix found within a conglomerate bed near the contact between the middle and upper zones of the lower member; E, desiccation cracks

along a bedding surface; F, outcrop image facing south depicting the distinct colour difference between the upper (left) and lower (right) members.

Figure 14. Compilation of main Mukpollo Formation sedimentary structures and rock types. A, channel fill composed of white quartz arenite (approximate height of individual 1.78 m); B, thinly laminated, very fine to fine dolomitic sandstone; C, alternating bands of light and dark, coarse-grained, well-rounded sandstone.

Figure 15. Compilation of main Kipalu Formation sedimentary structures and rock types. A, alternating layers of thinly laminated Fe-bearing argillaceous shale; B, thinly bedded, Fe-poor, grey-green argillite with thinly laminated, red-brown argillite caps; C, D, nodular horizons and lenses of granular iron formation; E, weathered granular iron formation surface. Red spheroids are largely composed of siderite (FeCO_3) fragments, while the silver blue clasts are a mixture of hematite and quartz (Morrow-Pollock 2021); F, fine-grained dolomitic siltstone preserving cross-stratification between two argillite beds.

Figure 16. A, tuff bed found within the Flaherty Formation; B, C, examples of the characteristic pillowed basalt flows.

Figure 17. Compilation of main Omarolluk Formation sedimentary structures and rock types. A, partial Bouma sequence typical of the turbidite facies division of Ricketts (1979, 1981); B, example of the calcareous concretions found throughout the lower member of the Omarolluk Formation; C, outcrop image depicting the bedding couplets that define the thin-bedded facies discussed in the text; D, a conglomerate bed composed of greywacke cobble clasts supported by very fine-grained grey sandstone; E, typical pattern of very thinly laminated dark grey sandstone overlain by very thinly laminated grey sandstone found near the top of the formation with larger scale sediment deformation structures (slump) creating convoluted bedding of very fine-grained sandstone. Slump folds on the scale of 1 m or larger are typical of the upper member.

Figure 18. Compilation of Loaf Formation sedimentary structures and rock types. A, thinly laminated very fine-grained feldspathic greywacke, characteristic of the lower member of the Loaf Formation; B, unidirectional ripples; C, reddish-pink arkose sandstone mixed with wisps of a darker red argillite; D, typical expression of a conglomerate bed composed of sub-rounded clasts of silty dolomicrite and dolomicrite; E, example of parallel laminations found within the mudstone-siltstone facies; F, trough cross-stratification.

Figure 19. Geological map of the community quarry by Steenkamp et al. (2016) and a carving of a polar bear made in 2019 by Samwillie Amagualik from carving stone of the Costello Formation and Haig intrusion. Yellow star denotes the location of the old Hudson Bay Company outpost location, while the pink star denotes the approximate location of the community quarry.

Figure 20. Compilation of common microbiota morphologies found within the Belcher Group. A–C, mat-forming microbiota of the Belcher Group from Plate 4 of Hofmann (1976); D, E, filamentous microfossils of probable cyanobacteria *Halythrix* sp. from the Paleoproterozoic Kasegalik Formation, Belcher Group, Canada (sample GSC 42769 in Hofmann 1976; photos from Butterfield (2015)), scale bar is 15 μm ; F, G, spherical microbiota (*Globophycus* sp.) found

within black chert of the Kasegalik or McLeary formations, images from Hofmann (1976), scale bar is 10 μm ; H, I, cyanobacterium *Eoentophysalis belcherensis*, H, pustule of cells showing multiple extra-cellular envelopes associated with cell division (sample GSC 43590; Butterfield 2015), I, type specimen of *E. belcherensis* (GSC 42770 from Hofmann 1976), scale bar 22 μm .

Figure 21. Composite schematic atmospheric O_2 curve from the 2.7 Ga to present with Paleoproterozoic large-scale geochemical and tectonic events and the Belcher Group depositional interval labeled. Modified from Partin (2023) with information from Catling and Zahnle (2020), Lyons et al. (2021), and Canfield et al. (2021). The Proterozoic was characterized by a wide range atmospheric O_2 that first rose to appreciable levels during the Great Oxidation Event and the subsequent Lomagundi–Jatuli Event. Atmospheric O_2 levels declined following these events in what is called the Deoxidation Event, which ushered in the low-oxygen conditions of the middle Proterozoic (1.8 to 0.8 Ga). The absolute O_2 levels in the Proterozoic Era are somewhat poorly constrained (represented by dashed curve) and a wide range of $p\text{O}_2$ values (represented by dashed boxes) is possible. Blue, red, green, and pink arrows representing lower or upper bounds of O_2 are from Catling and Zahnle (2020); magenta arrows representing probable O_2 increases (lacking upper/lower bounds) are from Lyons et al. (2021). The purple box represents the break-up of a super-craton (Kenorland), including the rifting of the Superior craton, and the teal box represents the assembly of the supercontinent Nuna, which includes the Trans-Hudson orogen affecting the margin of the Superior craton, as well as the deposition of the Belcher Group.

Figure 22. Stromatolite morphologies defined by examples found within the Kasegalik (A) and McLeary (B–D) formations. Box A depicts the commonly seen branching columnar stromatolite morphology characteristic of the *Minjaria* found within the Kasegalik Formation. Box B depicts small digitate stromatolite morphologies associated with *Linia* found within the middle member of the McLeary Formation. Box C depicts the columnar and dendroidal characteristics of the *Gymnosolen* group found with the upper member of the McLeary Formation. Box D depicts the characteristic conical shape of *Conophyton* found solely within the upper member of the McLeary Formation.

FIGURE 1

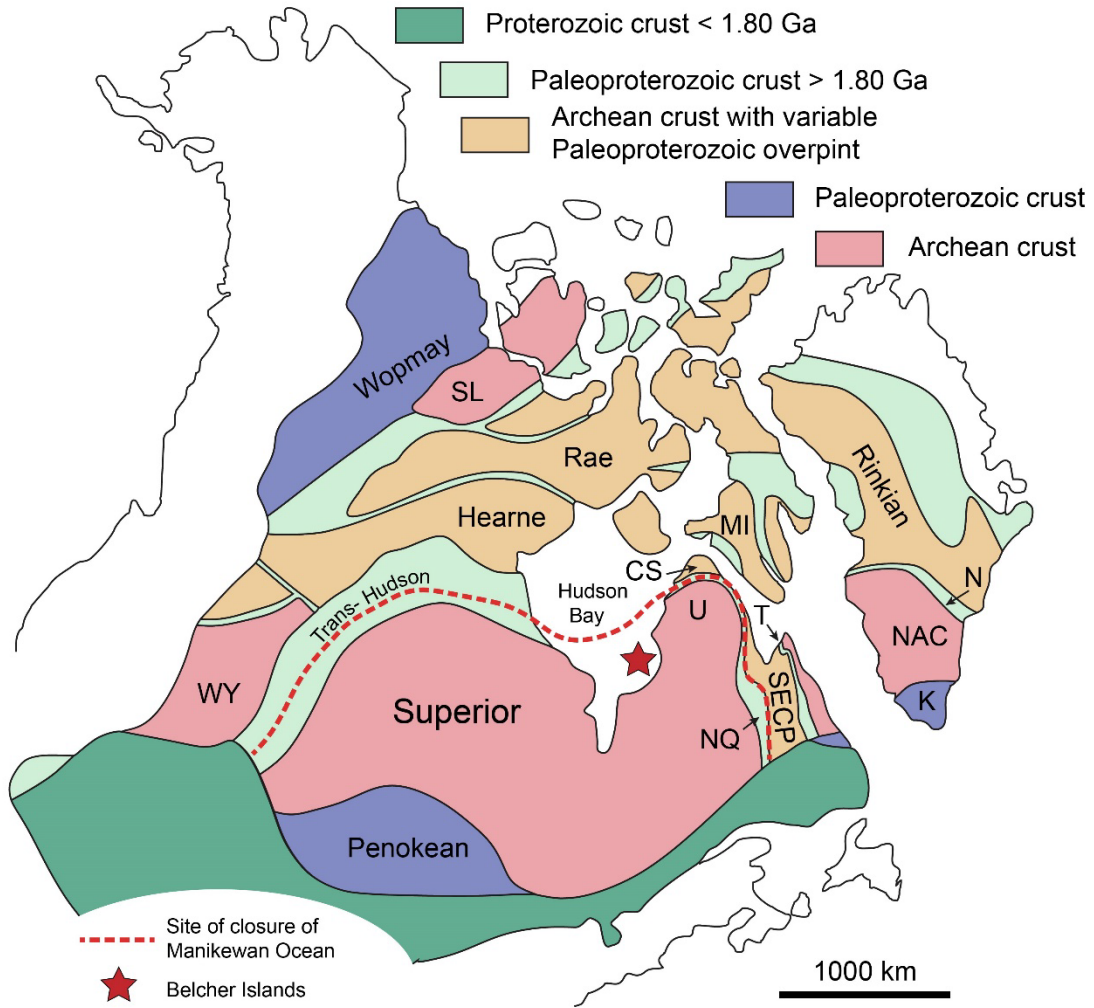


FIGURE 2 A-B

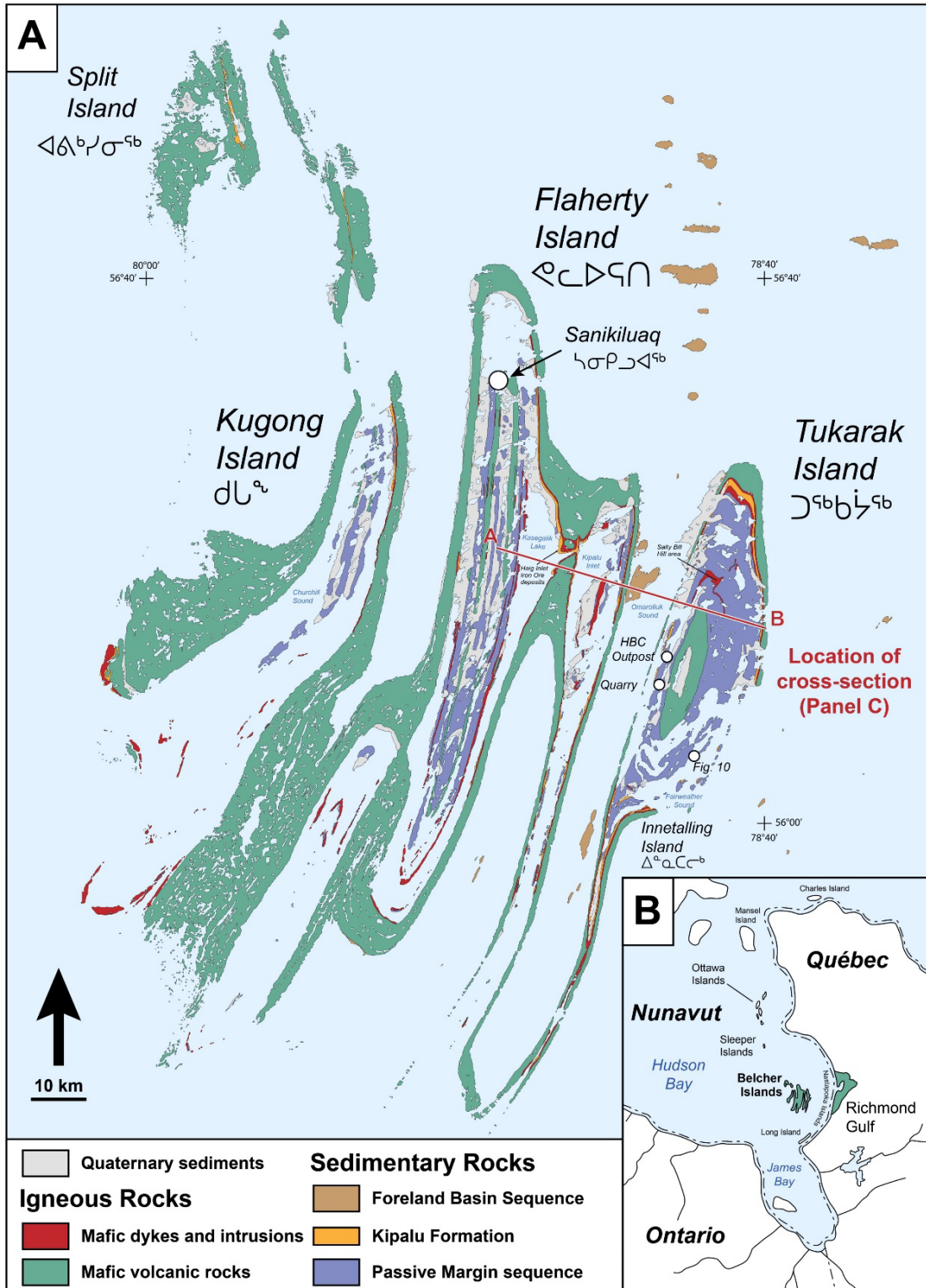


FIGURE 2 C

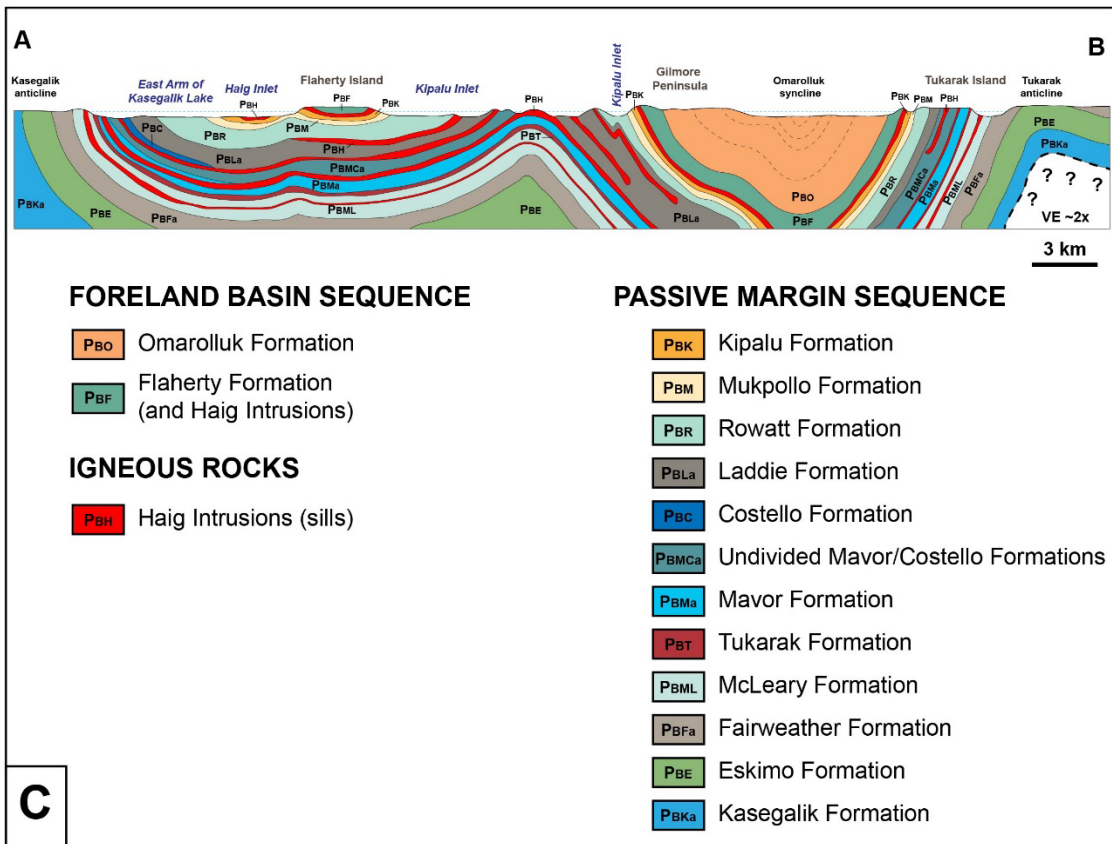


FIGURE 3

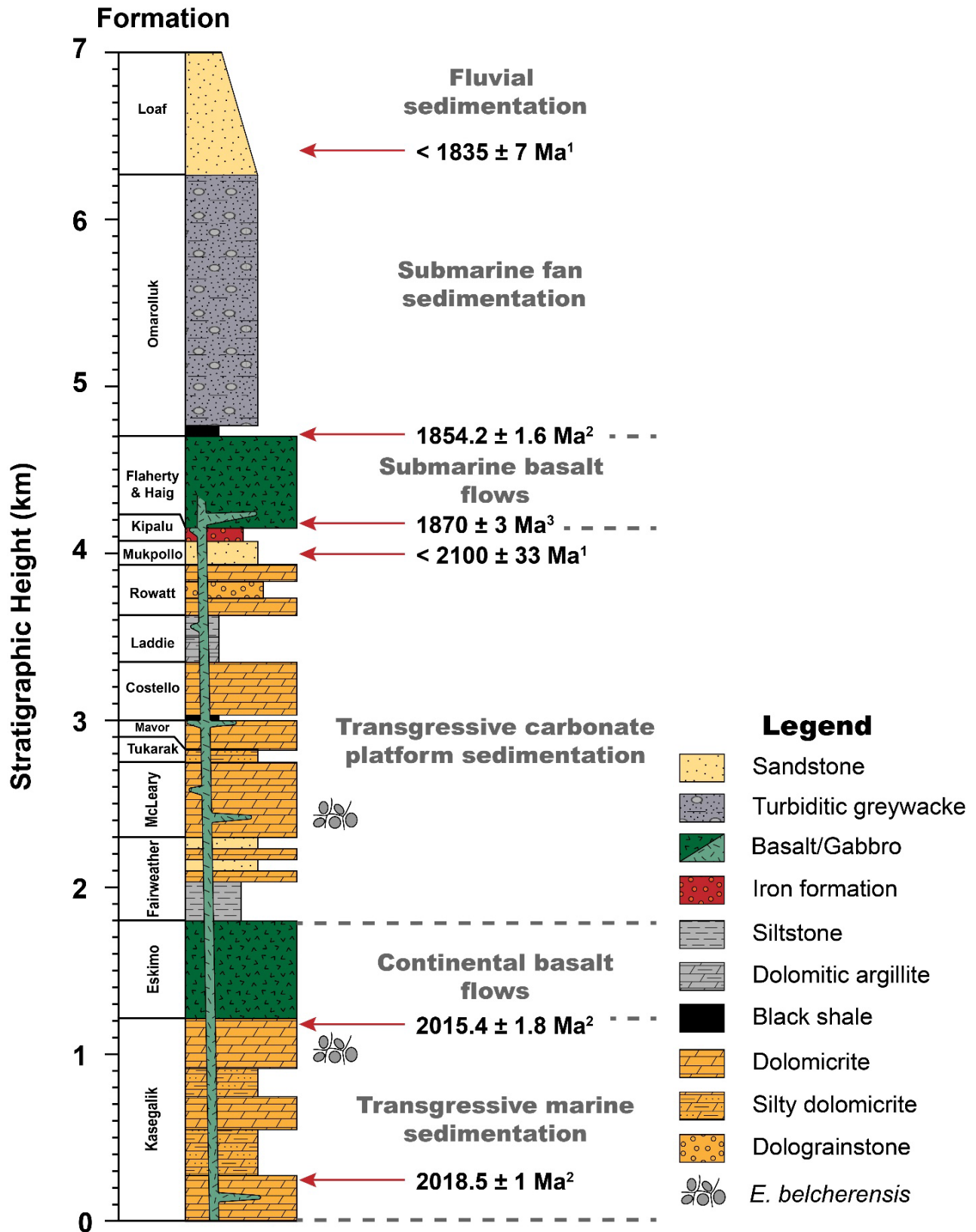


FIGURE 4

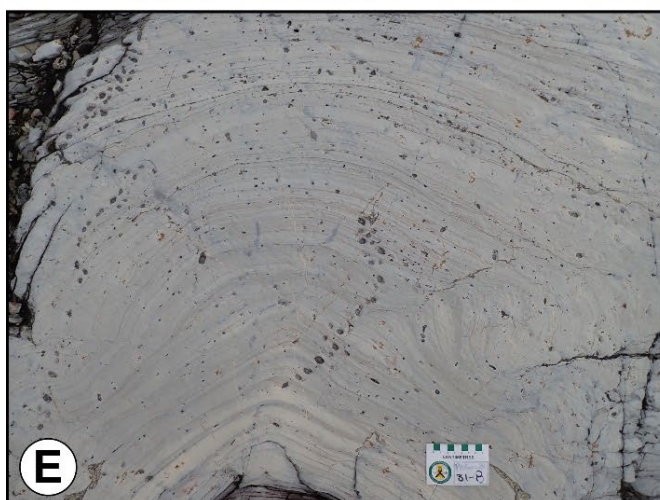


FIGURE 5

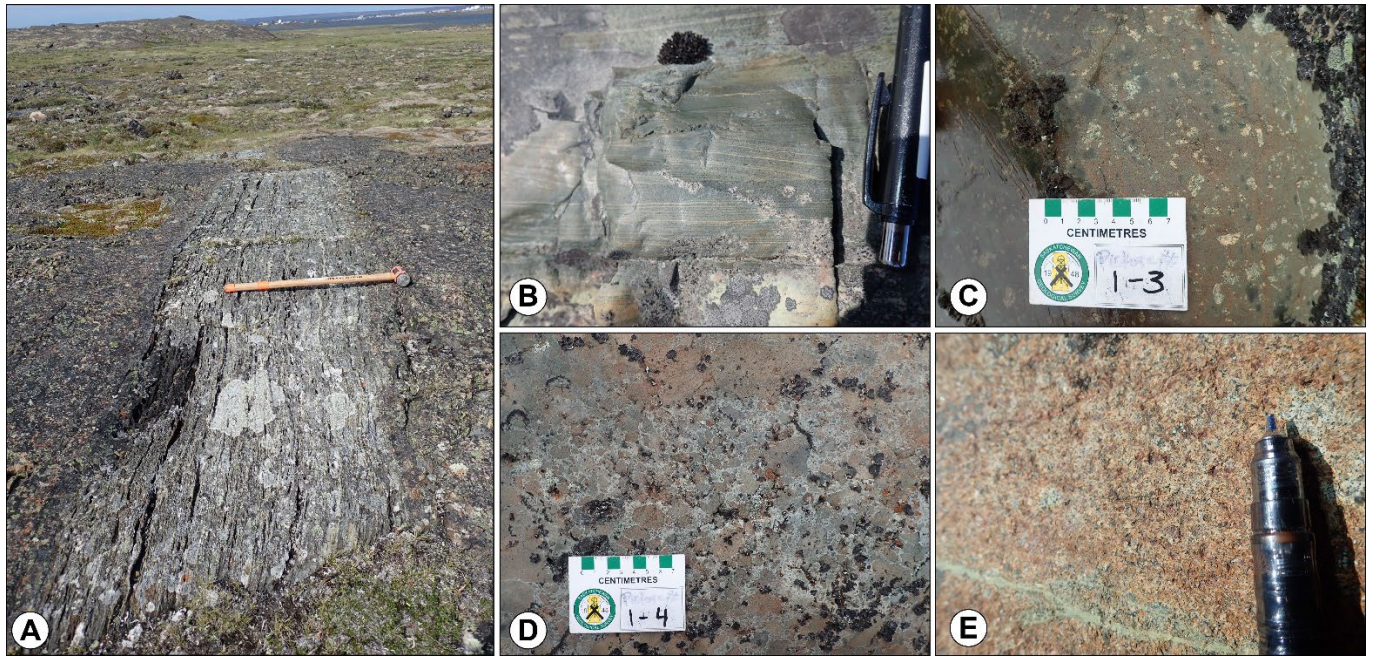


FIGURE 6

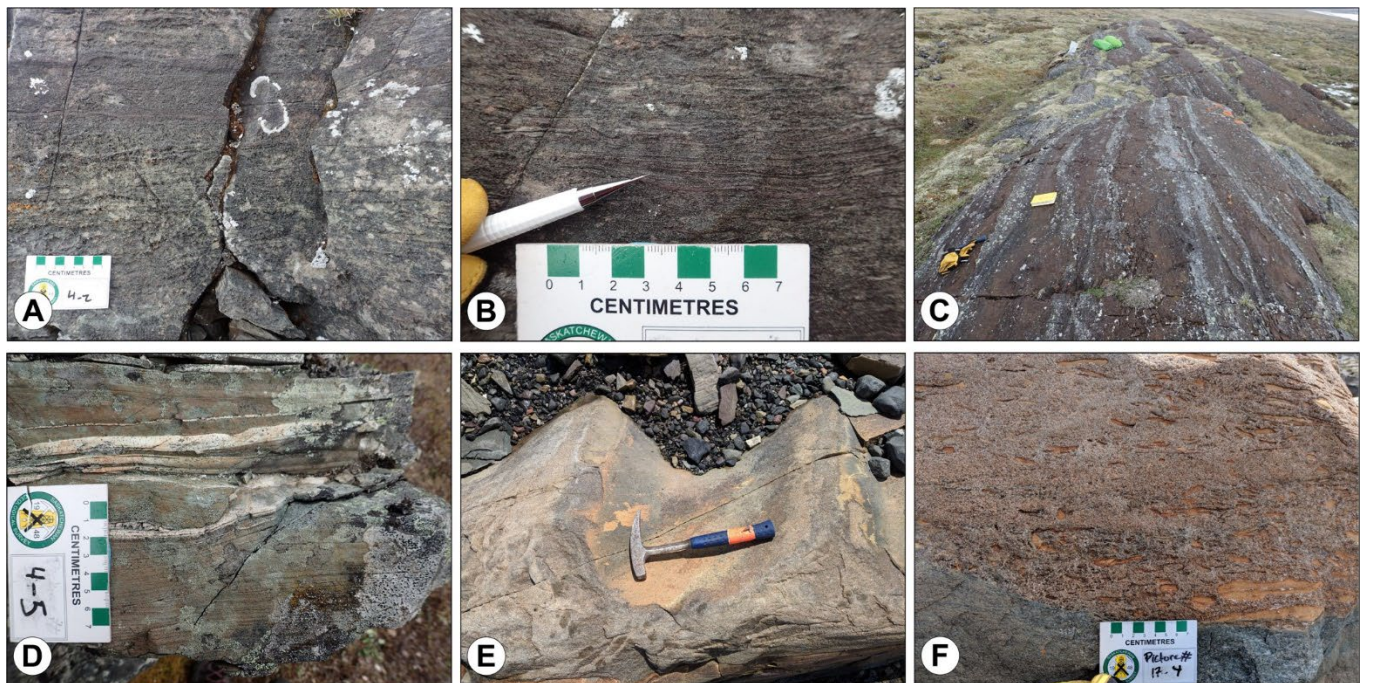


FIGURE 7



FIGURE 8

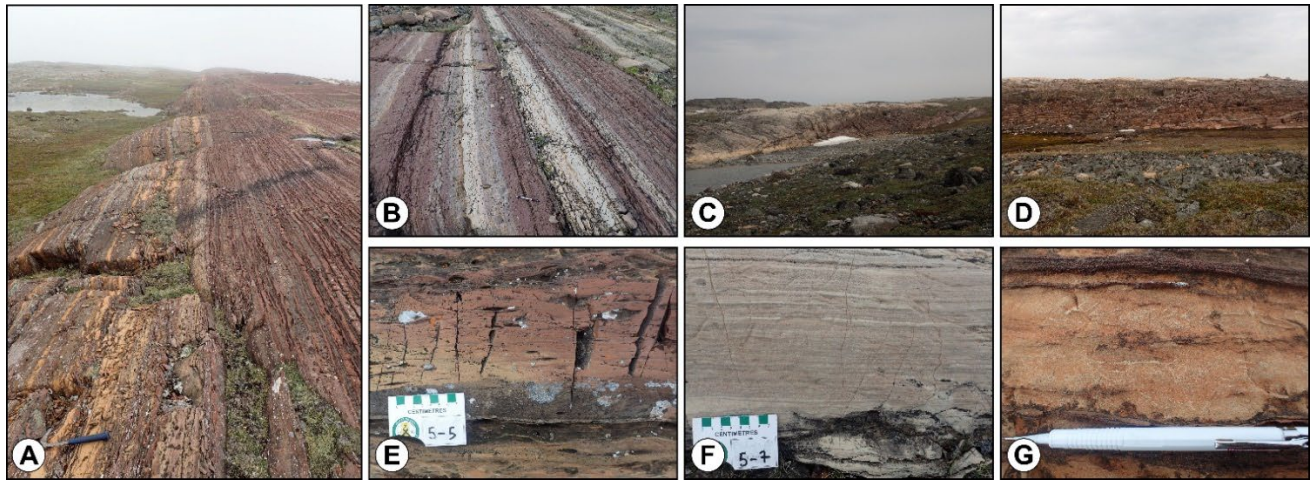


FIGURE 9

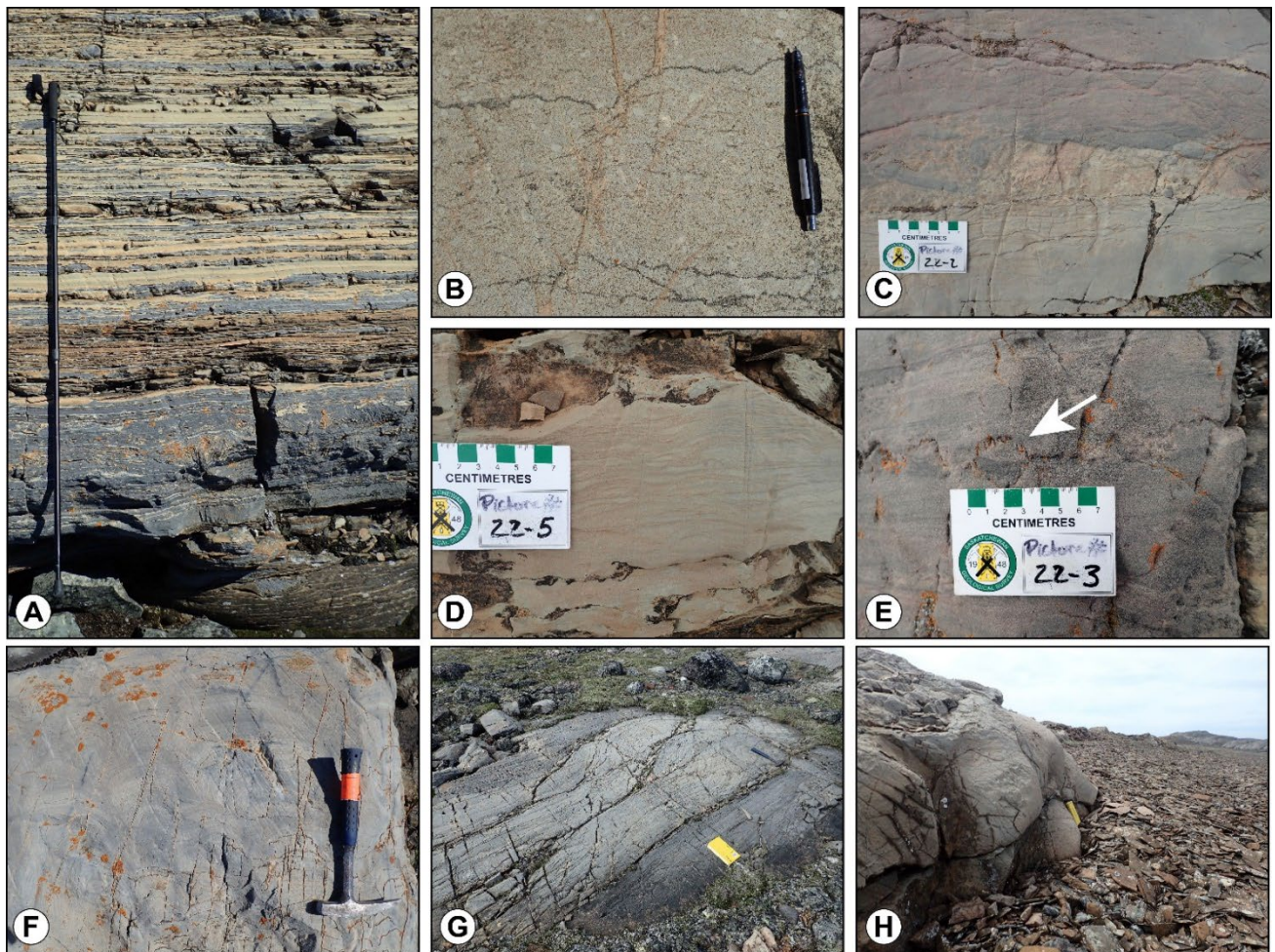


FIGURE 10

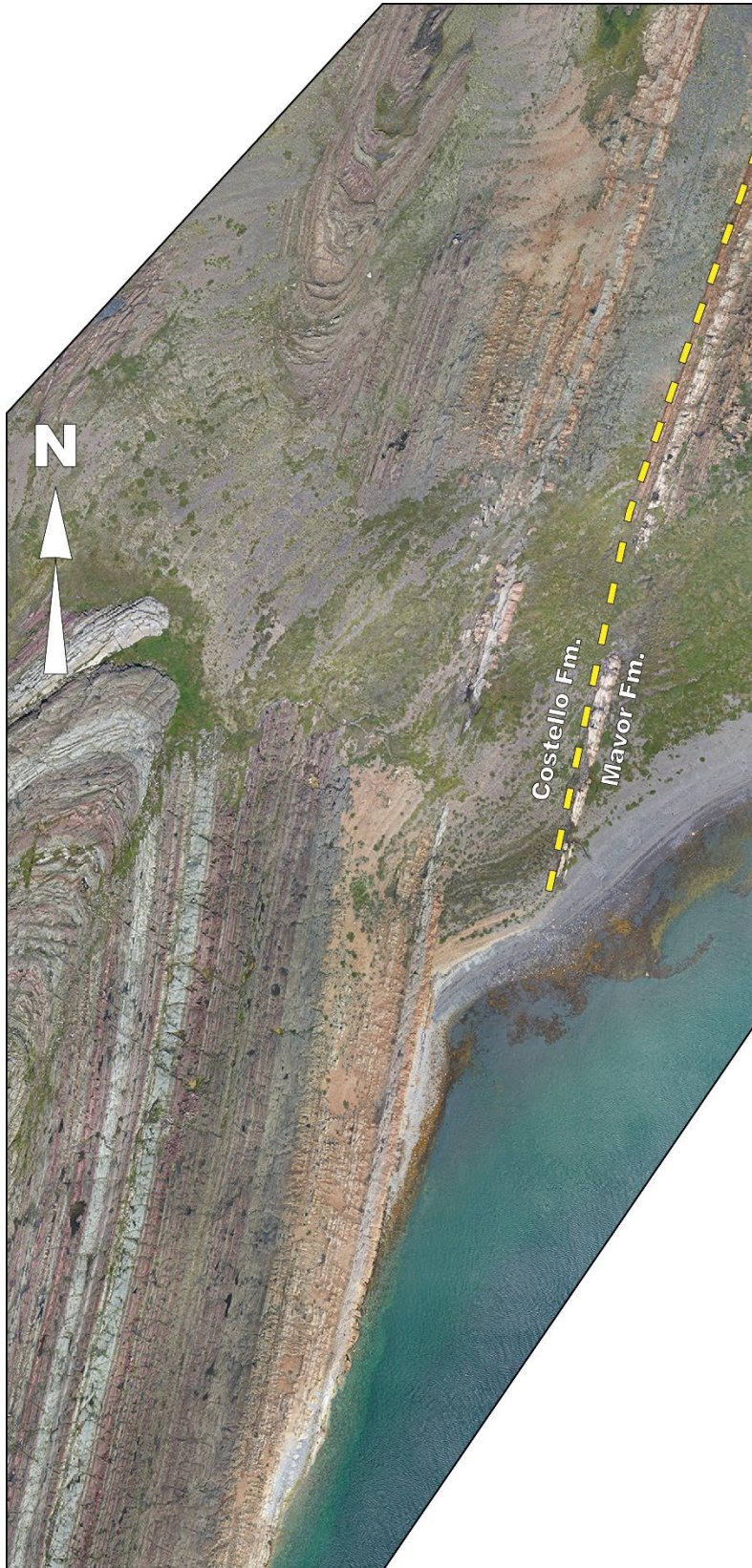


FIGURE 11



FIGURE 12



FIGURE 13

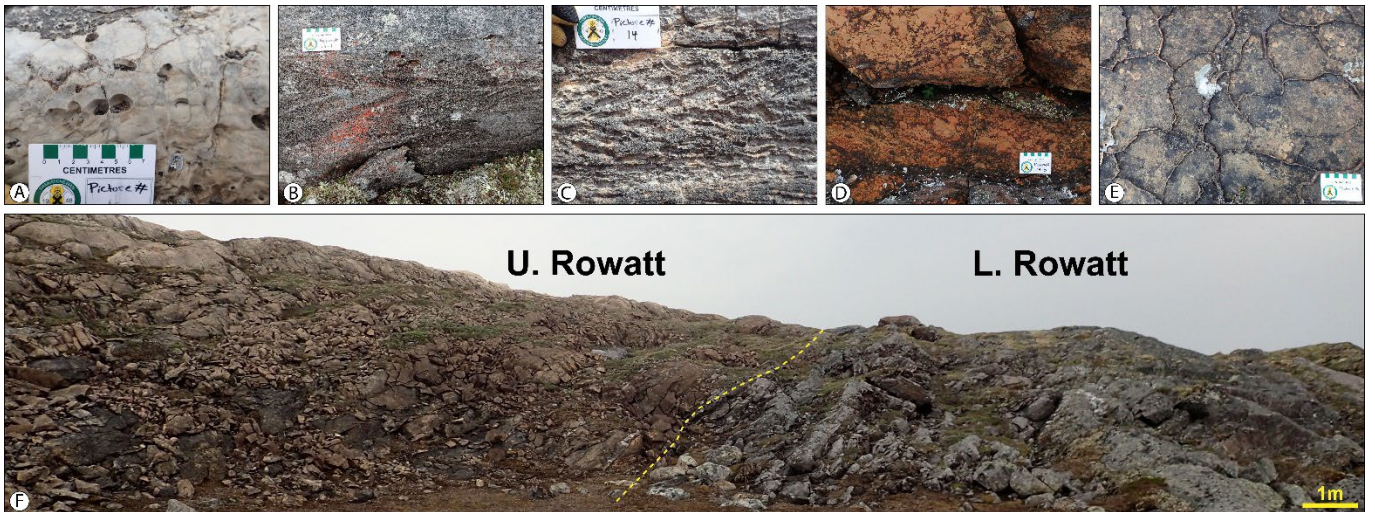


FIGURE 14

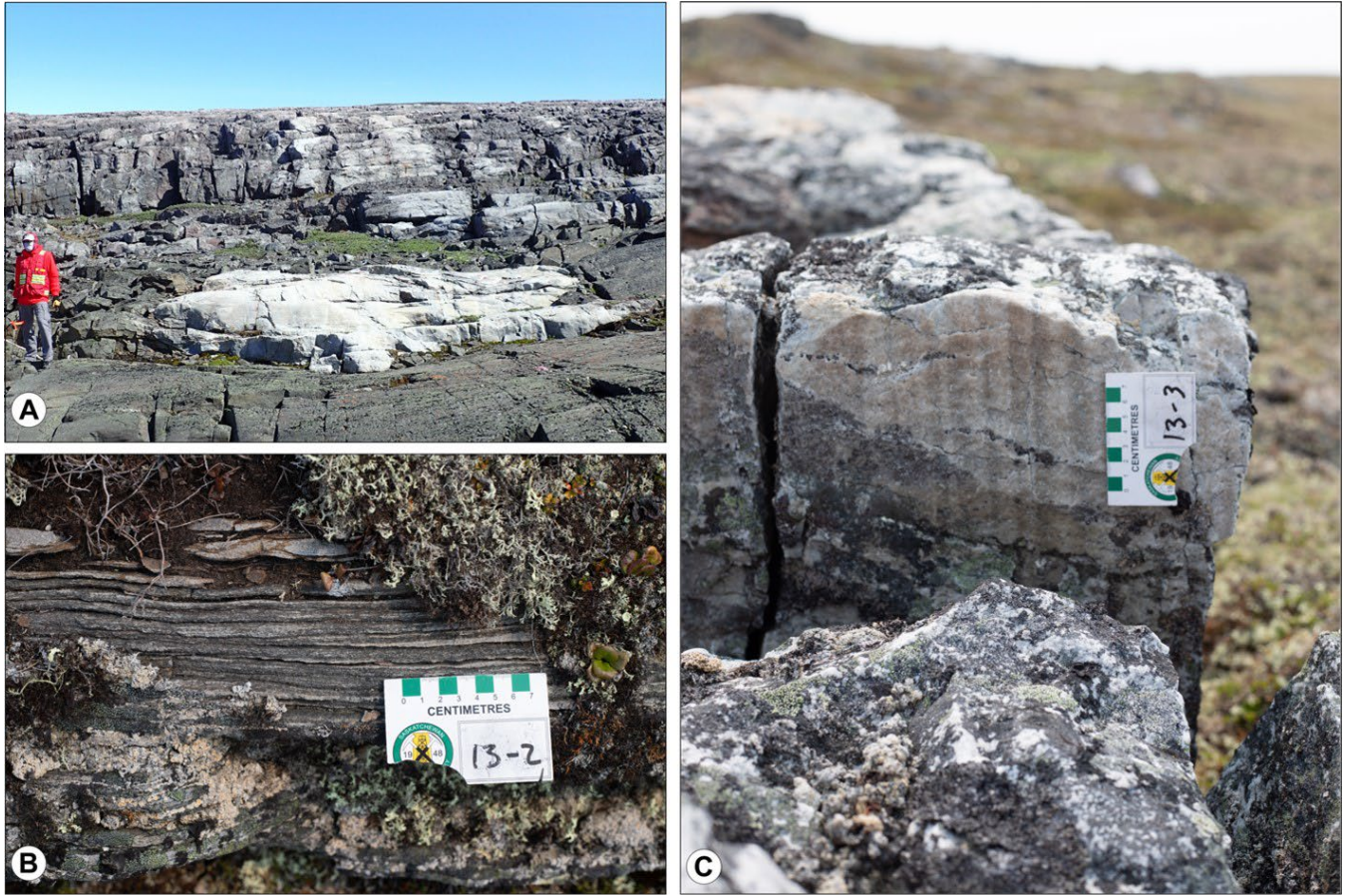


FIGURE 15

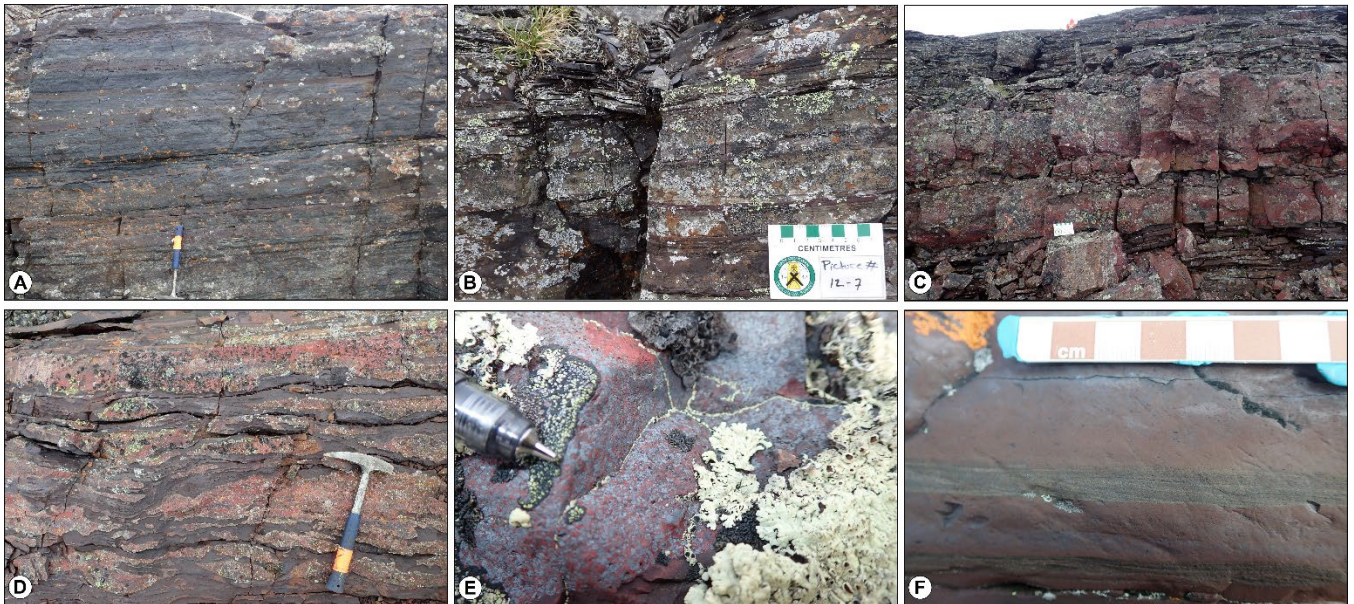


FIGURE 16



FIGURE 17

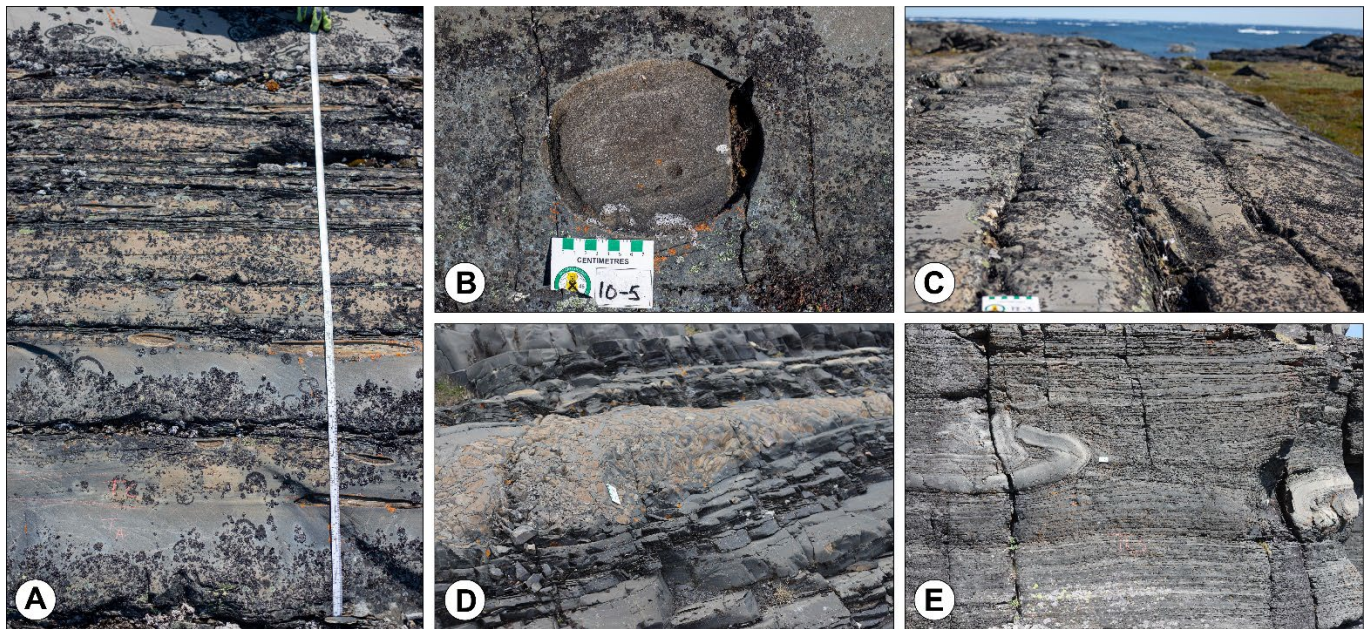


FIGURE 18

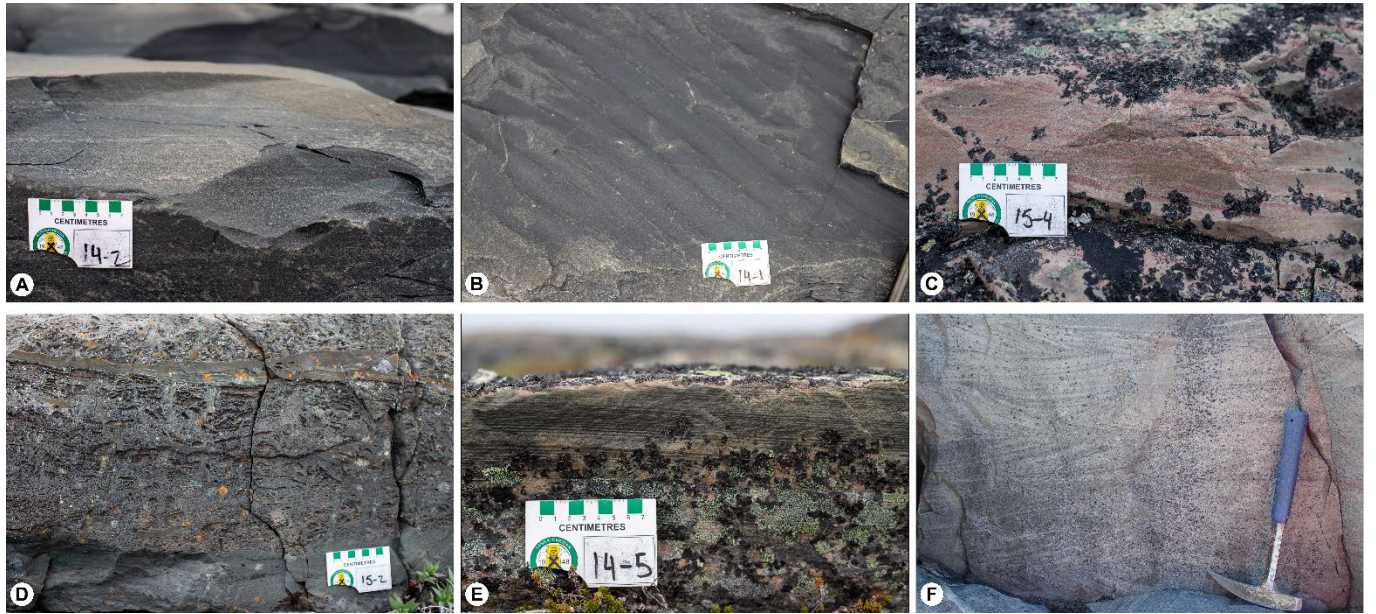


FIGURE 19

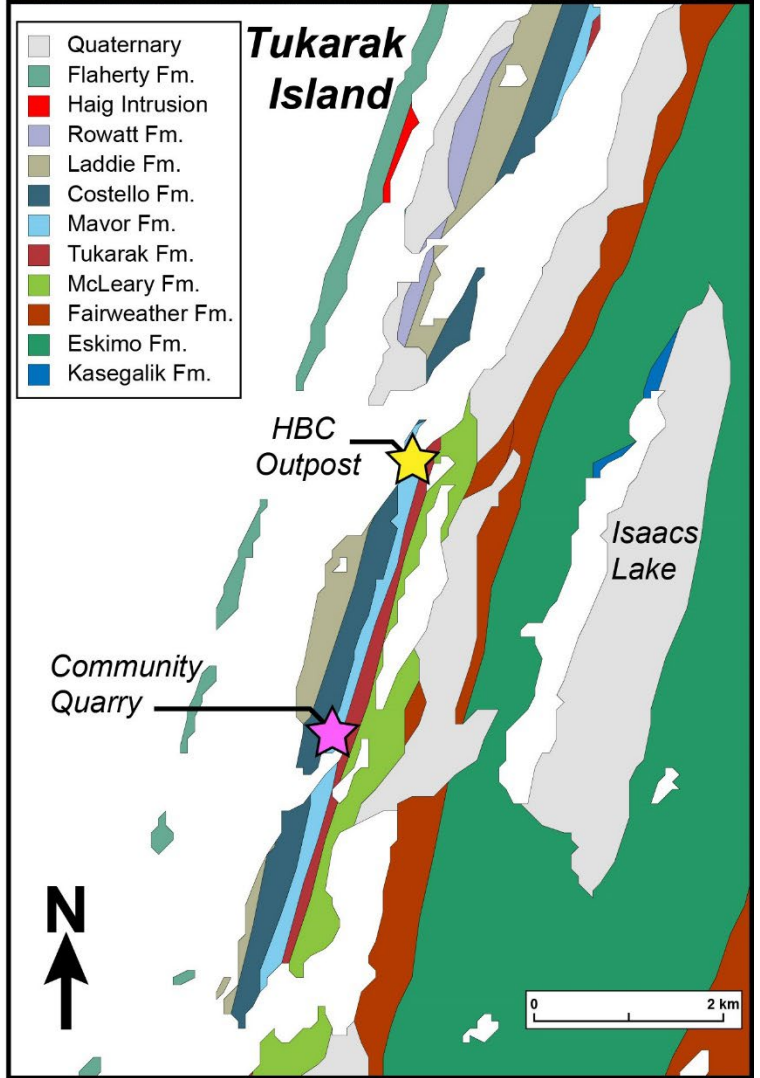
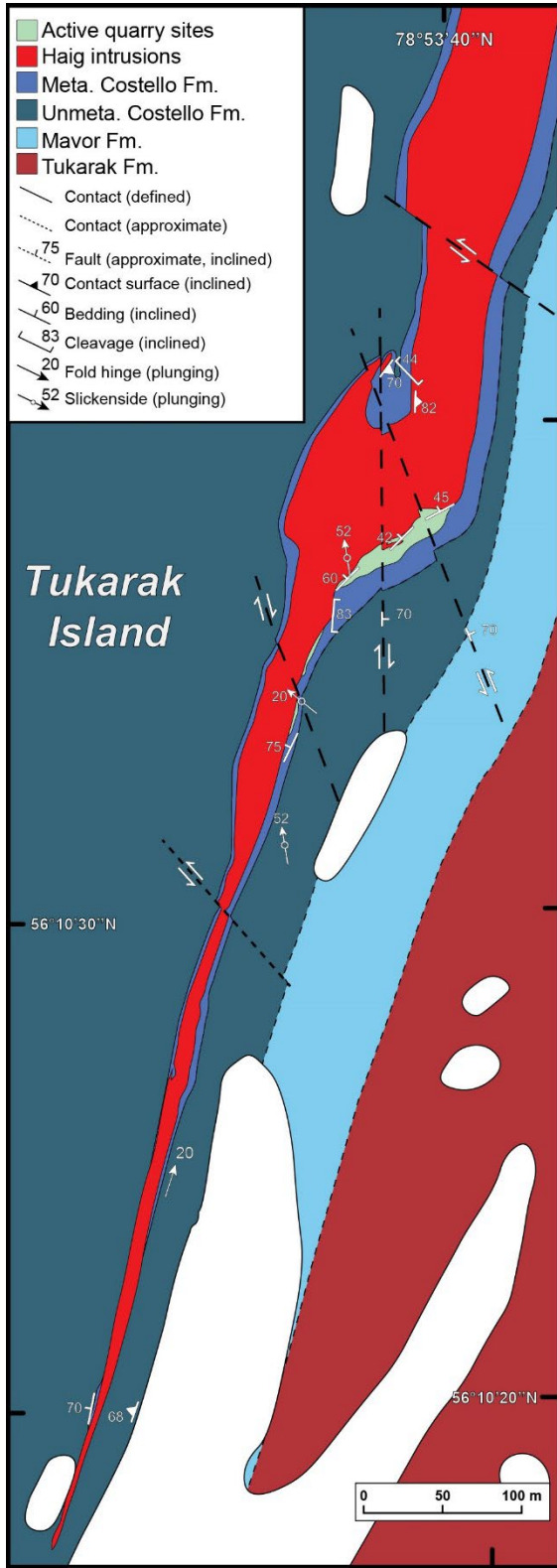


FIGURE 20

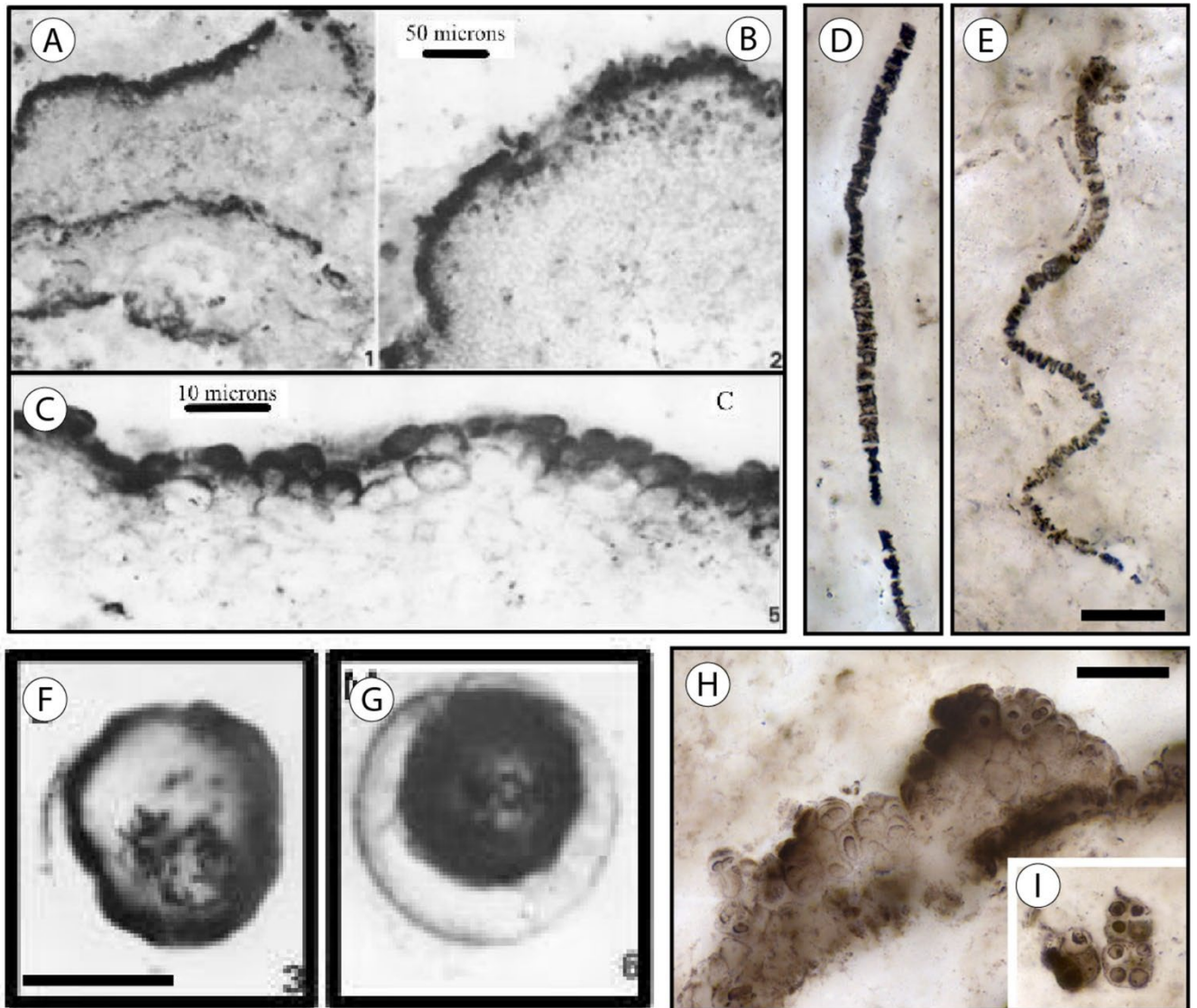


FIGURE 21

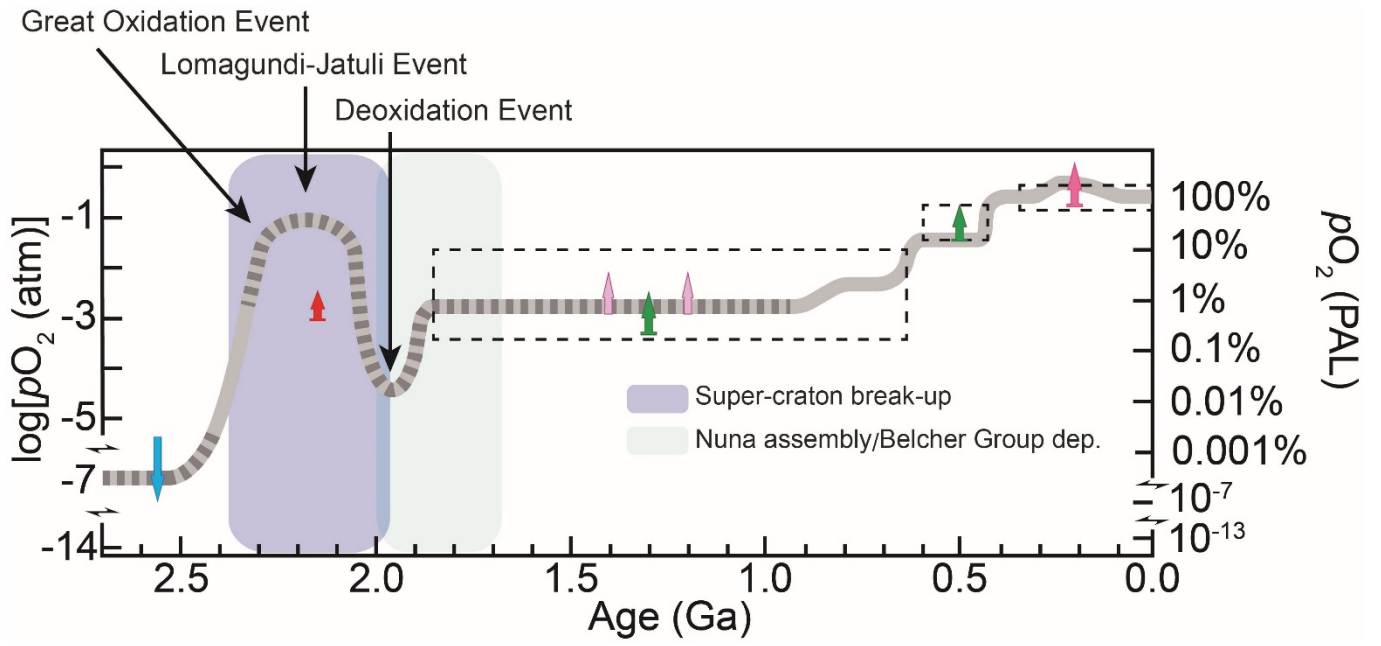


FIGURE 22

